

Functional Interaction between IKK and p73

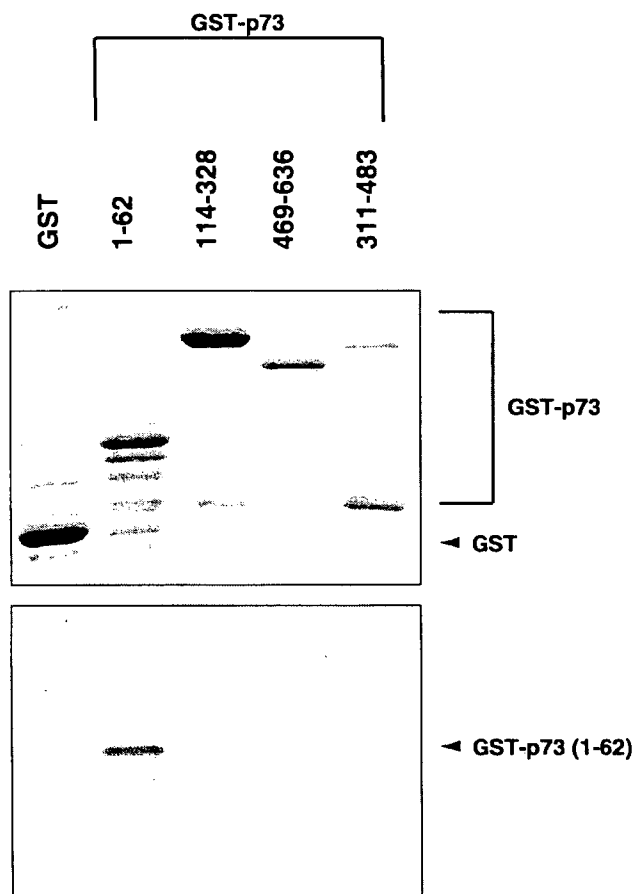


FIGURE 11. Active form of IKK- α phosphorylates p73 *in vitro*. Shown is the expression of GST-p73 deletion mutants. *Upper panel*, purified GST and the indicated GST-p73 deletion mutants were analyzed by SDS-PAGE, followed by Coomassie Brilliant Blue staining. *Lower panel*, shown are the results from the *in vitro* kinase reaction. Equal amounts of GST and the indicated GST-p73 deletion mutants were incubated with the active form of IKK- α in the presence of [γ - 32 P]ATP. After incubation, the reaction mixtures were separated by SDS-PAGE and subjected to autoradiography.

ately after birth because of uncontrolled hepatic apoptosis and exhibit an extensive defect in the activation of the NF- κ B pathway (49). Thus, it is likely that IKK- β is absolutely critical in the regulation of inducible I κ B degradation and the subsequent activation of the NF- κ B pathway in response to inflammatory stimuli, whereas IKK- α is not required for this process. Alternatively, other studies suggest that IKK- α is involved in NF- κ B activation through a second pathway that leads to the processing of the NF- κ B (p100) precursor (53, 54). Under our experimental conditions, IKK- β bound to p73 α as determined by immunoprecipitation analysis (data not shown); however, it failed to stabilize p73 α and to enhance its transactivation as well as pro-apoptotic activity. Unlike IKK- α , the amounts of endogenous nuclear IKK- β remained almost unchanged in response to CDDP. This is in good agreement with recent observations showing that IKK- α , but not IKK- β , has the ability to shuttle between the nucleus and cytoplasm (32). Taken together, our findings suggest that their functional divergence might be attributed at least in part to their differential interaction with p73.

Another finding of this study is that CDDP treatment results in a marked phosphorylation of I κ B- α in association with a significant down-regulation of cytoplasmic I κ B- α ; however, the

amounts of nuclear p65 remains unchanged. Consistent with these results, CDDP treatment did not enhance NF- κ B transcriptional activity in U2OS cells; however, p65 was induced to accumulate in the nucleus of L929 cells in response to TNF- α . Bian *et al.* (13) also reported that no change in NF- κ B-dependent transcriptional activation is observed in certain neuroblastoma cells in response to CDDP. It is therefore likely that, during the CDDP-dependent apoptotic process, the survival pathway mediated by NF- κ B might be impaired. As described previously (55), nuclear c-Abl is activated by DNA-damaging agents, including CDDP, but not by TNF- α , indicating that the differential behavior of p65 in response to CDDP or TNF- α might be due to the presence or absence of the activated form of c-Abl, respectively. In sharp contrast to CDDP, various anticancer agents, including camptothecin (topoisomerase I inhibition), paclitaxel (microtubule depolymerization inhibition), and doxorubicin (topoisomerase II inhibition), significantly induce the down-regulation of I κ B- α and promote the nuclear translocation of NF- κ B, followed by subsequent NF- κ B-dependent transcriptional activation (13, 56, 57). Considering that the cytoplasmic retention of NF- κ B by I κ B is the major molecular mechanism that controls its activity as well as cell fate determination (reviewed in Ref. 3), the CDDP-mediated attenuation of the nuclear accumulation of p65 might be required at least in part for apoptotic cell death in response to CDDP. In this connection, it is worth noting that NF- κ B promotes T cell survival by reducing the transcription of p73 following antigenic stimulation (27). Currently, it is not clear how the nuclear accumulation of p65 is blocked in cells exposed to CDDP, even though cytoplasmic I κ B- α is significantly decreased in our system. Future experiments will be necessary to clarify the underlying mechanistic details of this phenomenon.

It has been shown that p73 stability is regulated in a ubiquitination-dependent and -independent manner (43, 58). p73 is stabilized by coexpression with c-Abl or protein kinase C δ , which phosphorylates p73 at Tyr⁹⁹ or Ser²⁸⁹, respectively (16, 42). According to our results, IKK- α had the ability to stabilize p73, whereas the kinase-deficient mutant form of IKK- α does not, suggesting that the kinase activity of IKK- α is required for the stabilization of p73. As described previously (reviewed in Ref. 59), the amino acid sequence DSG Ψ XS (where Ψ is a hydrophobic amino acid and X is any amino acid) has been identified as a consensus motif for the IKK-dependent phosphorylation of I κ B proteins. During the search for a putative phosphorylation site(s) targeted by IKK within the amino acid sequence of p73 α , we failed to find a related motif. Of note, it has been shown that IKK- α , but not IKK- β and the kinase-deficient IKK- α mutant, phosphorylates histone H3 at Ser¹⁰, which has no IKK phosphorylation consensus sequence (33, 34). According to our *in vitro* kinase reaction, the active form of IKK- α has the ability to phosphorylate the N-terminal region of p73 α . Because IKK- α , but not the kinase-deficient IKK- α mutant, has the ability to stabilize p73 α , it is important to determine whether IKK- α can phosphorylate p73 in cells exposed to CDDP. In addition, it will be interesting to identify the signaling component(s) upstream of IKK- α that could receive the nuclear signal in response to CDDP-mediated DNA damage.

As described previously (60), the transcriptional coactivator p300 and CBP interact with p73 and enhance its function. Costanzo *et al.* (61) reported that DNA damage induces the acetylation of p73 by p300 in a c-Abl-dependent manner. In addition, Haupt *et al.* (62) found that p300-mediated acetylation results in p73 stabilization. It is worth noting that IKK- α , but not IKK- β , has the ability to interact with CBP (33). According to the previous results, IKK- α is required for the cytokine-induced phosphorylation and subsequent acetylation of histone H3. Although the precise molecular mechanism behind the IKK- α -dependent stabilization of p73 remains unknown, it is likely that a functional interaction might exist among c-Abl, p300/CBP, IKK- α , and p73. Our preliminary results suggest that the kinase-deficient form of c-Abl inhibits the IKK- α -dependent stabilization of p73 α (data not shown). This issue is currently under investigation in our laboratory.

Upon CDDP treatment, endogenous p73 α and p53 are significantly induced at the protein level in U2OS cells bearing wild-type p53 (45). Unlike p73, p53 is targeted for degradation by MDM2 through the ubiquitination-dependent proteasome pathway (reviewed in Ref. 38). It is well known that, in response to DNA damage, p53 is phosphorylated at multiple sites, including Ser¹⁵ and Ser²⁰, and that these phosphorylation events stimulate p53 stabilization by preventing the interaction with MDM2. Alternatively, Li *et al.* (63) found that HAUSP (herpesvirus-associated ubiquitin-specific protease) participates in the deubiquitination and subsequent stabilization of p53. Because the kinase-deficient IKK- α mutant inhibited the CDDP-induced stabilization of endogenous p73, but not of p53, the IKK- α -dependent stabilization appears to be highly specific to p73. Recently, Rossi *et al.* (64) reported that the HECT-type ubiquitin-protein isopeptide ligase Itch binds to and ubiquitinates p73, but not p53. Their study demonstrated that CDDP treatment results in a rapid reduction of Itch protein levels, indicating that Itch could contribute to the IKK- α -mediated stabilization of p73 α .

Furthermore, it has been shown that p53-dependent apoptosis requires the indirect contribution of at least one of the other p53 family members, p73 or p63, whereas p73 is sufficient in the absence of p53 to induce apoptosis (65). p53 is the most frequent target for genetic alterations in human cancers, leading to loss of its pro-apoptotic function (66). In addition to mutation of p53 itself, many cancers bearing wild-type p53 may harbor the other defects in the p53 pathway (reviewed in Ref. 38). In contrast to p53, p73 is infrequently mutated in many human cancers (67). Given the specific induction and activation of p73 by IKK- α , it is likely that the IKK- α -mediated induction of p73 substitutes for the downstream defects in the p53 pathway and/or enables p53 to cooperate with p73 to induce apoptosis.

Acknowledgments—We express our sincere appreciation to Drs. K. Takeshige and T. Muta for pELAM1-Luc. We give special thanks to Dr. Michael Karin for providing IKK- $\alpha^{-/-}$ MEFs. We thank S. Ono for excellent technical assistance.

REFERENCES

- Li, Q., and Verma, I. M. (2002) *Nat. Rev. Immunol.* 2, 725–734
- Karin, M. (2006) *Nature* 441, 431–436

- Karin, M., and Ben-Neriah, Y. (2000) *Annu. Rev. Immunol.* 18, 621–663
- Beg, A. A., and Baltimore, D. (1996) *Science* 274, 782–784
- Liu, Z., Hsu, G. H., Goeddel, D. V., and Karin, M. (1996) *Cell* 87, 565–576
- Wang, C.-Y., Mayo, M. W., and Baldwin, A. S., Jr. (1996) *Science* 274, 784–787
- Van Antwerp, D. J., Martin, S. J., Kafri, T., Green, D. R., and Verma, I. M. (1996) *Science* 274, 787–789
- Wang, C.-Y., Mayo, M. W., Korneluk, R. G., Goeddel, D. V., and Baldwin, A. S., Jr. (1998) *Science* 281, 1680–1683
- Wang, C.-Y., Cusack, J. C., Jr., Liu, R., and Baldwin, A. S., Jr. (1999) *Nat. Med.* 5, 412–417
- Cusack, J. C., Jr., Liu, R., Houston, M., Abendroth, K., Elliott, P. J., Adams, J., and Baldwin, A. S., Jr. (2001) *Cancer Res.* 61, 3535–3540
- Bayon, Y., Ortiz, M. A., Lopez-Hernandez, F. J., Gao, F., Karin, M., Pfahl, M., and Piedrafita, F. J. (2003) *Mol. Cell. Biol.* 23, 1061–1074
- Huang, Y., and Fan, W. (2002) *Mol. Pharmacol.* 61, 105–113
- Bian, X., McAllister-Lucas, I. M., Shao, F., Schumacher, K. R., Feng, Z., Porter, A. G., Castle, V. P., and Opipari, A. W. (2001) *J. Biol. Chem.* 276, 48921–48929
- Melino, G., De Laurenzi, V., and Vousden, K. H. (2002) *Nat. Rev. Cancer* 2, 605–615
- Gong, J., Costanzo, A., Yang, H.-Q., Melino, G., Kaelin, W. G., Jr., Levreno, M., and Wang, J. Y. (1999) *Nature* 399, 806–809
- Agami, R., Blandino, G., Oren, M., and Shaul, Y. (1999) *Nature* 399, 809–813
- Yuan, Z.-M., Shioya, H., Ishiko, T., Sun, X., Gu, J., Huang, Y. Y., Lu, H., Kharbanda, S., Weichselbaum, R., and Kufe, D. (1999) *Nature* 399, 814–817
- Yang, A., Walker, N., Bronson, R., Kaghad, M., Oosterwegel, M., Bonnin, J., Vagner, C., Bonnet, H., Dikens, P., Sharpe, A., McKeon, F., and Caput, D. (2000) *Nature* 404, 99–103
- Pozniak, C. D., Radinovic, S., Yang, A., McKeon, F., Kaplan, D. R., and Miller, F. D. (2000) *Science* 289, 304–306
- Stiewe, T., Zimmermann, S., Frilling, A., Esche, H., and Putzer, B. M. (2002) *Cancer Res.* 62, 3598–3602
- Grob, T. J., Novak, U., Maise, C., Barcaroli, D., Luthi, A. U., Pirnia, F., Hugli, B., Graber, H. U., De Laurenzi, V., Fey, M. F., Melino, G., and Tobler, A. (2001) *Cell Death Differ.* 8, 1213–1223
- Nakagawa, T., Takahashi, M., Ozaki, T., Watanabe, K., Todo, S., Mizuguchi, H., Hayakawa, T., and Nakagawara, A. (2002) *Mol. Cell. Biol.* 22, 2575–2585
- Zaika, A. I., Slade, N., Erster, S. H., Sansome, C., Joseph, T. W., Pearl, M., Chalas, E., and Moll, U. M. (2002) *J. Exp. Med.* 196, 765–780
- Wan, Y. Y., and DeGregori, J. (2003) *Immunity* 18, 331–342
- Tergaonkar, V., Pando, M., Vafa, O., Wahl, G., and Verma, I. M. (2002) *Cancer Cell* 1, 493–503
- Chang, N.-S. (2002) *J. Biol. Chem.* 277, 10323–10331
- Ryan, K. M., Ernst, M. K., Rice, N. R., and Vousden, K. H. (2000) *Nature* 404, 892–897
- Wu, H., and Lozano, G. (1994) *J. Biol. Chem.* 269, 20067–20074
- Sun, X., Shimizu, H., and Yamamoto, K. (1995) *Mol. Cell. Biol.* 15, 4489–4496
- Hellin, A. C., Calmant, P., Gielen, J., Bours, V., and Mervillie, M. P. (1998) *Oncogene* 16, 1187–1195
- Fujioka, S., Schmidt, C., Scwab, G. M., Li, Z., Pelicano, H., Peng, B., Yao, A., Niu, J., Zhang, W., Evans, D. B., Abbruzzese, J. L., Huang, P., and Chiao, P. J. (2004) *J. Biol. Chem.* 279, 27549–27559
- Birbach, A., Gold, P., Binder, B. R., Hofer, E., de Martin, R., and Schmid, J. (2002) *J. Biol. Chem.* 277, 10842–10851
- Yamamoto, Y., Verma, U. N., Prajapati, S., Kwak, Y.-T., and Gaynor, R. B. (2003) *Nature* 423, 655–659
- Anest, V., Hanson, J. L., Cogswell, P. C., Steinbrecher, K. A., Strahl, B. D., and Baldwin, A. S., Jr. (2003) *Nature* 423, 659–663
- Nickerson, J. A., Krockmalnic, G., Wan, K. M., Turner, C. D., and Penman, S. (1992) *J. Cell Biol.* 116, 977–987
- Ben-Yehoyada, M., Ben-Dor, I., and Shaul, Y. (2003) *J. Biol. Chem.* 278, 34475–34482
- Xirodimas, D., Staville, M. K., Edling, C., Lane, D. P., and Lain, S. (2001)

Functional Interaction between IKK and p73

- Oncogene* **20**, 4972–4983
38. Vousden, K. H., and Lu, X. (2002) *Nat. Rev. Cancer* **2**, 594–604
 39. Verma, U. N., Yamamoto, Y., Prajapati, S., and Gaynor, R. B. (2004) *J. Biol. Chem.* **279**, 3509–3515
 40. Muta, T., and Takeshige, K. (2001) *Eur. J. Biochem.* **268**, 4580–4589
 41. Hehner, S. P., Hofmann, T. G., Ratter, F., Dumont, A., Droge, W., and Schmitz, M. L. (1998) *J. Biol. Chem.* **273**, 18117–18121
 42. Ren, J., Datta, R., Shioya, H., Li, Y., Oki, E., Biedermann, V., Bharti, A., and Kufe, D. (2002) *J. Biol. Chem.* **277**, 33758–33765
 43. Lee, C.-W., and La Thangue, N. B. (1999) *Oncogene* **18**, 4171–4181
 44. Nakamura, Y., Ozaki, T., Niizuma, H., Ohira, M., Kamijo, T., and Nakagawara, A. (2007) *Biochem. Biophys. Res. Commun.* **354**, 892–898
 45. Ling, L., Cao, Z., and Goeddel, D. V. (1998) *Proc. Natl. Acad. Sci. U. S. A.* **95**, 3792–3797
 46. Kim, E.-J., Park, J.-S., and Um, S.-J. (2002) *J. Biol. Chem.* **277**, 32020–32028
 47. Mittnacht, S., and Weinberg, R. A. (1991) *Cell* **65**, 381–393
 48. Zandi, E., Chen, Y., and Karin, M. (1998) *Science* **281**, 1360–1363
 49. Li, Q., Van Antwerp, D., Mercurio, F., Lee, K. F., and Verma, I. M. (1999) *Science* **284**, 321–325
 50. Takeda, K., Takeuchi, O., Tsujimura, T., Itami, S., Adachi, O., Kawai, T., Sanjo, H., Yoshikawa, K., Terada, N., and Akira, S. (1999) *Science* **284**, 313–316
 51. Hu, Y., Baud, V., Delhase, M., Zhang, P., Deerinck, T., Ellisman, M., Johnson, R., and Karin, M. (1999) *Science* **284**, 316–320
 52. Li, Q., Lu, Q., Hwang, J. Y., Buscher, D., Lee, K. F., Izpisua-Belmonte, J. C., and Verma, I. M. (1999) *Genes Dev.* **13**, 1322–1328
 53. Senftleben, U., Cao, Y., Xiao, G., Greten, F. R., Krahn, G., Bonizzi, G., Chen, Y., Hu, Y., Fong, A., Sun, S. C., and Karin, M. (2001) *Science* **293**, 1495–1499
 54. Pomerantz, J. L., and Baltimore, D. (2002) *Mol. Cell* **10**, 693–695
 55. Kharbanda, S., Ren, R., Pandey, P., Shafman, T. D., Feller, S. M., Weichselbaum, R. R., and Kufe, D. W. (1995) *Nature* **376**, 785–788
 56. Huang, Y., Johnson, K. R., Norris, J. S., and Fan, W. (2000) *Cancer Res.* **60**, 4426–4432
 57. Huang, T. T., Wuerzberger-Davis, S. M., Scufzer, B. J., Shumway, S. D., Kurama, T., Boothman, D. A., and Miyamoto, S. (2000) *J. Biol. Chem.* **275**, 9501–9509
 58. Ohtsuka, T., Ryu, Y. H., Minamishima, Y. A., Ryo, A., and Lee, S. W. (2003) *Oncogene* **22**, 1678–1687
 59. Karin, M. (1999) *Oncogene* **18**, 6867–6874
 60. Zeng, X., Li, X., Miller, A., Yuan, Z., Yuan, W., Kwok, R. P. S., Goodman, R., and Lu, H. (2000) *Mol. Cell. Biol.* **20**, 1299–1310
 61. Costanzo, A., Merlo, P., Pediconi, N., Fulco, M., Sartorelli, V., Cole, P. A., Fontemaggi, G., Fanciulli, M., Schiltz, L., Blandino, G., Balsano, C., and Levrero, M. (2002) *Mol. Cell* **9**, 175–186
 62. Haupt, Y., Maya, R., Kazaz, A., and Oren, M. (1997) *Nature* **387**, 296–299
 63. Li, M., Chen, D., Shiloh, A., Luo, J., Nikolaev, A. Y., Qin, J., and Gu, W. (2002) *Nature* **416**, 643–653
 64. Rossi, M., De Laurenzi, V., Munarriz, E., Green, D. R., Liu, Y. C., Vousden, K. H., Cesareni, G., and Melino, G. (2005) *EMBO J.* **24**, 836–848
 65. Flores, E. R., Tsai, K. Y., Crowley, D., Sen Gupta, S., Yang, A., McKeon, F., and Jacks, T. (2002) *Nature* **416**, 560–564
 66. Hollstein, M., Soussi, T., Thomas, G., von Breen, M., and Bartsch, H. (1997) *Recent Results Cancer Res.* **143**, 369–389
 67. Ikawa, S., Nakagawara, A., and Ikawa, Y. (1999) *Cell Death Differ.* **6**, 1154–1161

NFBD1/MDC1 Associates with p53 and Regulates Its Function at the Crossroad between Cell Survival and Death in Response to DNA Damage^{*[S]}

Received for publication, December 13, 2006, and in revised form, May 2, 2007. Published, JBC Papers in Press, May 29, 2007, DOI 10.1074/jbc.M611412200

Mitsuru Nakanishi^{†§1}, Toshinori Ozaki^{†1}, Hideki Yamamoto[‡], Takayuki Hanamoto[‡], Hironobu Kikuchi[‡], Kazushige Furuya[‡], Masahiro Asaka[§], Domenico Delia[¶], and Akira Nakagawara^{‡2}

From the [†]Division of Biochemistry, Chiba Cancer Center Research Institute, Chiba 260-8717, Japan, the [§]Department of Gastroenterology, Hokkaido University School of Medicine, Sapporo 060-8638, Japan, and the [¶]Department of Experimental Oncology, Istituto Nazionale Tumori, 20133 Milan, Italy

NFBD1/MDC1, which belongs to the BRCT superfamily, has an anti-apoptotic activity and contributes to the early cellular responses to DNA damage. Here we found that NFBD1 protects cells from apoptotic cell death by inhibiting phosphorylation of p53 at Ser-15 under steady state as well as early phase of DNA damage, thereby blocking its transcriptional and pro-apoptotic activities. During late phase of DNA damage, a remarkable reduction of NFBD1 was observed in dying but not in surviving A549 cells bearing wild-type p53. Small interference RNA-mediated knockdown of the endogenous NFBD1 resulted in an increase in sensitivity to adriamycin in A549 cells but not in p53-deficient H1299 cells. Immunoprecipitation and luciferase reporter analyses demonstrated that NFBD1 binds to the NH₂-terminal region of p53 and strongly inhibits its transcriptional activity. Additionally, BRCT domains, which can interact with p53, reduced the adriamycin-induced phosphorylation levels of p53 at Ser-15 and also suppressed the transcriptional activity of p53. Thus, our present findings strongly suggest that NFBD1 plays an important role in the decision of cell survival and death after DNA damage through the regulation of p53.

found in a variety of cellular proteins such as BRCA1, 53BP1, and RAD9, which are involved in DNA repair and/or DNA damage signaling pathways (1–3). Although the functional role of the BRCT domain is currently unclear, the early works indicated that the BRCT domains of BRCA1 act as a transactivator (4, 5). Consistent with this notion, the point mutations detected within the BRCT domains of BRCA1 markedly inhibited its transcriptional activity (4, 5), and BRCA1 was a component of RNA polymerase II holoenzyme (6). Alternatively, the BRCT domains function as protein-protein interaction modules (7). For example, the BRCT domains of BRCA1 as well as 53BP1 were required for the interaction with p53 (8, 9).

NFBD1/MDC1 (nuclear factor with BRCT domain 1/mediator of DNA damage checkpoint protein 1) is a large nuclear protein bearing three characteristic structural domains, including an NH₂-terminal forkhead-associated (FHA) domain, an internal PST (proline/serine/threonine-rich) repeat domain, and tandem repeat of COOH-terminal BRCT domains (10–14). We have initially reported that NFBD1 acts as a nuclear transcriptional factor with an anti-apoptotic function (11). In accordance with our results, siRNA-mediated knockdown of NFBD1 led to a significant increase in the number of apoptotic cells (15). In addition, the elimination of NFBD1 expression increased the sensitivity to irradiation (16). These observations indicate that NFBD1 has an anti-apoptotic function; however, the precise molecular mechanisms behind the anti-apoptotic effect of NFBD1 remain to be explored.

Previous studies strongly suggest that NFBD1 is closely involved in early cellular responses to genotoxic stress. Upon DNA damage, NFBD1 was phosphorylated in an ATM/Chk2-dependent manner and cooperated with γ H2AX to recruit DNA repair proteins to the sites of DNA damage (12–14). Consistent with this notion, NFBD1 was associated with the DNA double strand break repair MRN complex, including MRE11, RAD50, and NBS1, and also co-localized with the MRN complex as well as γ H2AX at the nuclear foci in response to DNA damage (12, 14, 15, 17). Deletion analysis revealed that the FHA and BRCT domains of NFBD1 are required for the binding to the MRN complex and γ H2AX, respectively (15). Furthermore, siRNA-mediated knockdown of NFBD1 led to a significant decrease in the number of irradiation-induced NBS1 foci (14), and the FHA and BRCT domains of NFBD1 were responsible for the formation of irradiation-induced nuclear foci contain-

The BRCA1 carboxyl terminus (BRCT)³ domain is defined by distinct hydrophobic clusters of amino acids and is often

* This work was supported in part by a grant-in-aid from the Ministry of Health, Labor, and Welfare for Third Term Comprehensive Control Research for Cancer, a grant-in-aid for Cancer Research from the Ministry of Health, Labor, and Welfare of Japan, a grant-in-aid from the Ministry of Education, Culture, Sports, Science and Technology, Japan, and a grant from Uehara Memorial Foundation. The costs of publication of this article were defrayed in part by the payment of page charges. This article must therefore be hereby marked "advertisement" in accordance with 18 U.S.C. Section 1734 solely to indicate this fact.
[S] The on-line version of this article (available at <http://www.jbc.org>) contains supplemental Fig. 1.

¹ Both authors contributed equally to this work.

² To whom correspondence should be addressed. Tel: 81-43-264-5431; Fax: 81-43-265-4459; E-mail: akiranak@chiba-cc.jp.

³ The abbreviations used are: BRCT, BRCA1 carboxyl terminus; ADR, adriamycin; ATM, ataxia-telangiectasia-mutated; CDDP, cisplatin; CPT-11, camptothecin; DAPI, 4,6-diamidino-2-phenylindole; FHA, forkhead-associated; GAPDH, glyceraldehyde-3-phosphate dehydrogenase; GFP, green fluorescent protein; HRP, horseradish peroxidase; MRN, MRE11-RAD50-NBS1; NFBD1, nuclear factor with BRCT domain 1; NF- κ B, nuclear factor- κ B; NRS, normal rabbit serum; NOX, nocodazole; PST, proline/serine/threonine-rich; PTX, paclitaxel; RT, reverse transcription; siRNA, small interference RNA; VP-16, etoposide; E3, ubiquitin-protein isopeptide ligase; MTT, 3-(4,5-dimethylthiazol-2-yl) 2,5-diphenyl-tetrazolium bromide.

Functional Interaction between NFBD1/MDC1 and p53

ing NFBD1 (12–14). Lou *et al.* (18) described that the PST domain of NFBD1 binds to Ku/DNA-dependent protein kinase, and this interaction is critical for the efficient irradiation-induced autophosphorylation of DNA-dependent protein kinase.

p53 is a nuclear transcription factor with a pro-apoptotic function. In response to a wide variety of cellular stresses, including genotoxic stress, p53 is phosphorylated, and its half-life is dramatically prolonged. During the DNA damage-induced apoptosis, p53 is directly phosphorylated at Ser-15 and Ser-20 by ATM and Chk2, respectively (19–23). Such phosphorylation events contribute to the increased stability and activity of p53 by facilitating its dissociation from E3 ubiquitin protein ligase MDM2 (reviewed in Ref. 24).

In this study, we demonstrate that NFBD1 abrogates the adriamycin (ADR)-mediated apoptosis through the inhibition of the transcriptional as well as pro-apoptotic activity of p53. Our present findings strongly suggest that NFBD1 plays a pivotal role in the regulation of cell survival and death after DNA damage.

EXPERIMENTAL PROCEDURES

Cell Culture and Transfection—COS7 and HEK293T cells were maintained in Dulbecco's modified Eagle's medium containing 10% heat-inactivated fetal bovine serum (Invitrogen) and penicillin (100 IU/ml)/streptomycin (100 µg/ml). A549 and H1299 cells were grown in RPMI 1640 medium with the same supplements. Where indicated, cells were treated with ADR. For transfection, COS7 cells were transfected with the indicated expression plasmids using FuGENE 6 transfection reagent (Roche Applied Science), except for A549 and H1299 cells, for which Lipofectamine 2000 transfection reagent (Invitrogen) was used.

Cell Survival Assay—Cell viability was determined by a modified 3-(4,5-dimethylthiazol-2-yl) 2,5-diphenyl-tetrazolium bromide (MTT) assay. In brief, A549 cells were cultured overnight at 5×10^3 cells per well in a 96-well plate, and then exposed to ADR. At the indicated time periods after the treatment with ADR, 10 µl of MTT solution was added to each culture, and the mixture was maintained for another 3 h at 37 °C. The absorbance readings for each well were carried out at 570 nm using the microplate reader (model 450; Bio-Rad).

Isolation of RNA and RT-PCR—Total RNA was prepared from A549 cells using the RNeasy Mini kit (Qiagen, Valencia, CA) according to the manufacturer's protocol. A total of 1 µg of total RNA was used to generate cDNAs with random primers by SuperScript II reverse transcriptase (Invitrogen). PCR amplification was carried out under standard conditions with rTaq DNA polymerase (Takara, Ohtsu, Japan). The primer sets used in this study were designed based on the cDNA sequences corresponding to each of the genes by using Primer3 software (Whitehead Institute). The primer sequences were as follows: p21^{WAF1}, 5'-ATGAAATTCACCCCCTTCC-3' (sense) and 5'-CCCTAGGCTGTGCTCACTTC-3' (antisense); p53, 5'-GTCCAGATGAAGCTCCAGAG-3' (sense) and 5'-CAAGGCCTCATTCAGCTCTC-3' (antisense); NFBD1, 5'-AGCAACCCAGTTGTCATTC-3' (sense) and 5'-AGCGCTGCTGAGACTTCTTC-3' (antisense); BAX, 5'-AGAGGATGATTGCCG-

CGT-3' (sense) and 5'-CAACCACCCTGGTCTTGGAT-3' (antisense); PUMA, 5'-CTGTGAATCCTGTGCTCTGC-3' (sense) and 5'-TCCTCCCTCTTCCGAGATTT-3' (antisense); NOXA, 5'-CTGGAAGTCGAGTGTGCTACT-3' (sense) and 5'-TCAGGTTCCCTGAGCAGAAGAG-3' (antisense); and GAPDH, 5'-ACCTGACCTGCCGTCTAGAA-3' (sense) and 5'-TCCACCACCCTGTTGCTGTA-3' (antisense). PCR products were separated by 1.5% agarose gel electrophoresis and stained with ethidium bromide.

Antibody Production—The cDNA sequence encoding the NH₂-terminal region of human NFBD1 (amino acid residues 1–150) was subcloned into the bacterial expression plasmid pGEX-4T-2 (Amersham Biosciences), expressed in *Escherichia coli* DH5α, and purified with a glutathione-Sepharose 4B column. The antiserum against NFBD1 was produced by immunizing rabbit with the above purified glutathione S-transferase fusion protein.

Construction of the Deletion Mutants of NFBD1—NFBD1 cDNA fragment encoding NH₂-terminal FHA domain (amino acid residues 2–141), central PST domain (amino acid residues 788–1645), or COOH-terminal BRCT domains (amino acid residues 1858–2068) was amplified by PCR with the following primers: 5'-GAATTCGAGGACACCCAGGCTATT-3' and 5'-GAGCTCAGTCCTCTGTTTCCCGTC-3' or 5'-CCGGAATTCGACCAACATCCAGAGAGC-3' and 5'-TCGCCGGCAGTGAGTTCTAGTCTCCG-3' or 5'-GAATTCAGCCTCCGACGCACCAA-3' or 5'-GAGCTCAGTACTACTGTAGTGGT-3', respectively. PCR primers also included 5'-EcoRI and 3'-XhoI or 5'-EcoRI and 3'-NotI restriction sites (boldface and underlined) to aid cloning. PCR products were then inserted in-frame into the appropriate restriction sites of the pcDNA3-FLAG to give pcDNA3-FLAG-FHA, pcDNA3-FLAG-PST, and pcDNA3-FLAG-BRCT.

RNA Interference—To construct an expression plasmid for siRNA against NFBD1, two DNA oligonucleotides were designed to produce 19-nucleotide siRNA. Oligonucleotides used are as follows: 5'-CCCCAGCTCGAGCCTTCCACTTCTTCAAGAGAGAAGTGGAAGGCTCGAGCTTTTTTGGAAAC-3' and 5'-TCGAGTTTCCAAAAAGCTCGAGCCTTCCACTTCTCTTGAAGAAGTGGAAGGCTCGAGCTGGGAGCT-3'. These two oligonucleotides were mixed in equimolar amounts and annealed under the standard conditions. The annealed oligonucleotide was inserted into the SacI and XhoI restriction sites of pcDNA3 derivative in which the cytomegalovirus promoter was replaced with the *H1* promoter.

Generation of Stable A549 Cell Lines—To establish stable cell lines expressing siRNA against p53, A549 cells were stably transfected with pSUPER-p53 (OligoEngine, Seattle, WA) or with the backbone plasmid, and cultured in the presence of G418 (400 µg/ml). Two weeks after the selection in G418, drug-resistant clones were isolated and allowed to proliferate in medium containing G418.

Immunoblotting—Protein lysates (50 µg) were separated by 10% SDS-PAGE, electrotransferred onto Immobilon-P membranes (Millipore, Bedford, MA), and probed with anti-p53 (DO-1; Oncogene Research Products, Cambridge, MA), anti-FLAG (M2; Sigma), anti-BAX (6A7; eBioscience, San Diego), anti-GFP (1E4; MBL, Nagoya, Japan), anti-p21^{WAF1} (H-164;

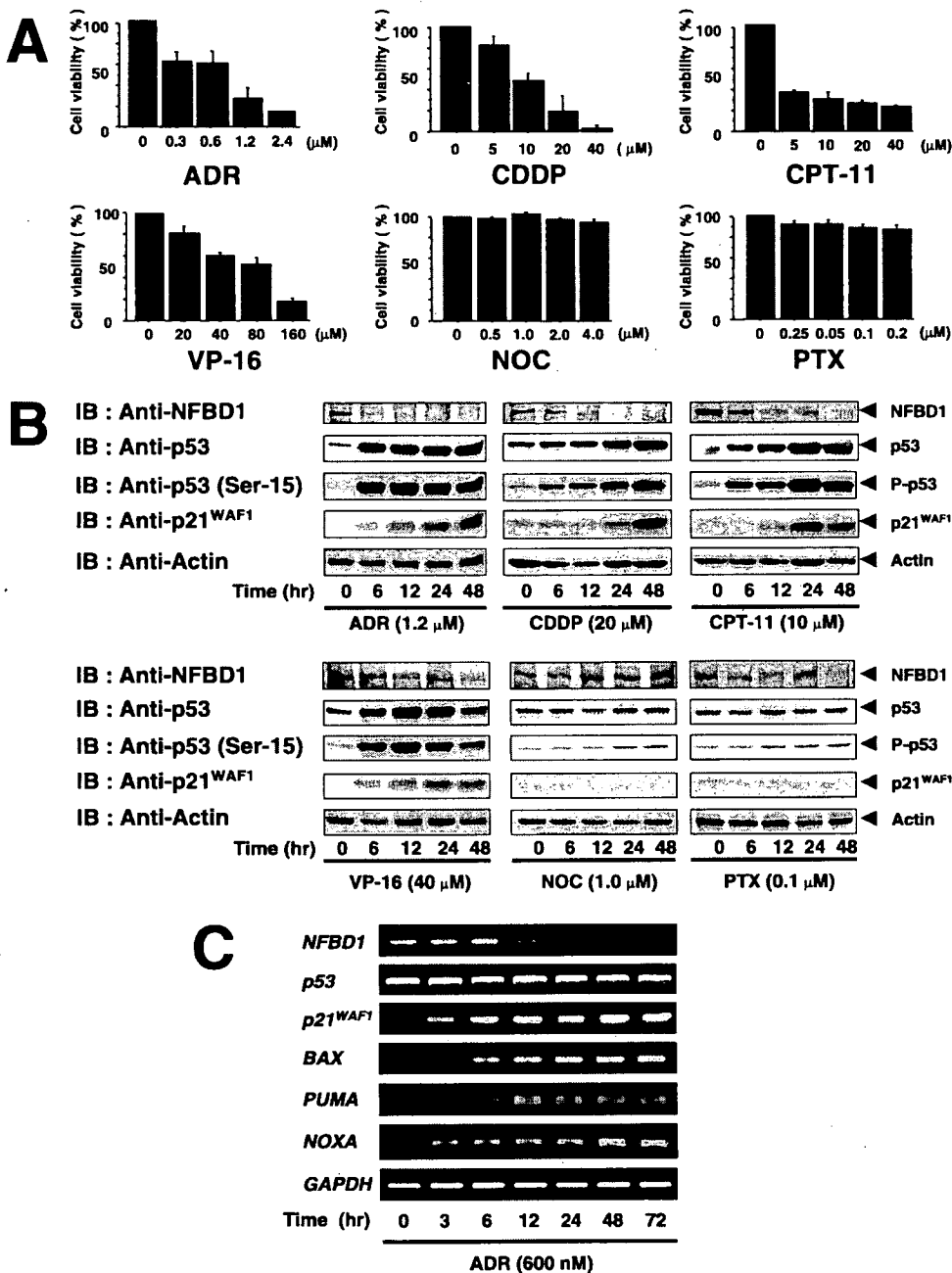


FIGURE 1. Down-regulation of NFBD1 in association with the induction of p53 in response to genotoxic stresses. *A*, cell survival assays. A549 cells were treated with various genotoxic agents, including ADR, CDDP, CPT-11, and VP-16 or with the nongenotoxic agents such as nocodazole (NOC) and PTX. Forty eight hours after treatment, cell viability was determined by MTT assays. Data are presented as the mean values \pm S.D. of three independent experiments. *B*, down-regulation of NFBD1 following DNA damage. A549 cells bearing wild-type p53 were exposed to ADR (1.2 μ M), CDDP (20 μ M), CPT-11 (10 μ M), VP-16 (40 μ M), nocodazole (1 μ M), or PTX (0.1 μ M). At the indicated time points after the drug treatment, whole cell lysates were prepared and analyzed by immunoblotting (IB) with the indicated antibodies. Immunoblotting for actin is shown as control for equal protein loading. *C*, RT-PCR analysis. A549 cells were treated with 600 nM ADR. At the indicated time periods after the treatment with ADR, total RNA was prepared and subjected to RT-PCR. GAPDH was used as an internal control.

Santa Cruz Biotechnology, Santa Cruz, CA), anti-actin (20–33; Sigma), anti-p53 (Ser-15) (16G8; Cell Signaling, Beverly, MA), or with anti-PUMA (Abcam, Cambridge, UK) antibody, followed by an incubation with horseradish peroxidase-conjugated goat anti-mouse or rabbit secondary antibody (Jackson ImmunoResearch, West Grove, PA). Protein-antibody com-

plexes were visualized by enhanced chemiluminescence with the ECL system (Amersham Biosciences).

Immunoprecipitation—Precleared whole cell lysates were immunoprecipitated with normal rabbit serum (NRS) or with the anti-NFBD1 antibody, and the immunoprecipitates were recovered using protein G-Sepharose beads (Amersham Biosciences). After extensive washing with the lysis buffer, bound proteins were eluted out by boiling in SDS sample buffer and processed for immunoblotting with the indicated antibodies.

In Vitro Binding Assay—³⁵S-labeled FLAG-tagged FHA, PST, and BRCT domains were transcribed and translated *in vitro* using the TNT T7 QuickCoupled transcription/translation system (Promega, Madison, WI). For pulldown assay, cell lysates prepared from COS7 cells were incubated with the radio-labeled proteins for 2 h at 4 °C. After incubation, the reaction mixture was immunoprecipitated with anti-p53 antibody (DO-1) for 2 h at 4 °C, followed by an incubation with protein G-Sepharose beads. The immunoprecipitates were recovered by brief centrifugation, washed with the lysis buffer, boiled in SDS sample buffer, and separated by 10% SDS-PAGE. After gel drying, radio-labeled proteins were visualized by autoradiography.

Indirect Immunofluorescence—For immunofluorescence, fixation was in 4% paraformaldehyde and permeabilization was in 0.2% Triton X-100. Coverslips were with anti-p53 (DO-1), anti-p53 (Ser-15) (16G8) or with anti-NFBD1 antibody. Cells were imaged by confocal microscope (Olympus, Tokyo, Japan).

Apoptosis Assay—A549 cells were transiently co-transfected with the constant amount of the expression plasmid for green fluorescence protein (GFP) together with or without

the NFBD1 expression plasmid or the expression plasmid for siRNA against NFBD1. Twenty four hours after transfection, cells were treated with ADR or left untreated and incubated for another 24 h. Transfected cells were identified by the presence of green fluorescence. To verify apoptosis, cell nuclei were stained with DAPI to reveal nuclear condensation and frag-

Functional Interaction between NFBD1/MDC1 and p53

mentation. The number of GFP-positive cells with apoptotic nuclei was scored.

Luciferase Reporter Assay—H1299 cells were transiently co-transfected with the indicated expression plasmids and reporter constructs. Forty eight hours post-transfection, whole cell lysates were prepared, and luciferase activity was assessed using a Promega dual luciferase assay system. The firefly luminescence signal was normalized based on the *Renilla* luminescence signal. The results were obtained from at least three sets of transfection and were presented as the mean \pm S.D.

RESULTS

Down-regulation of NFBD1 in Response to a Variety of Genotoxic Agents—To explore the role of NFBD1 during the DNA damage response, we examined the expression kinetics of NFBD1 in human lung carcinoma A549 cells exposed to a variety of genotoxic agents, including ADR, camptothecin (CPT-11), cisplatin (CDDP), or etoposide (VP-16). In addition to the genotoxic agents, we also investigated the effect of nongenotoxic agents such as nocodazole (NOC) and paclitaxel (PTX) on NFBD1. A549 cells were exposed to the indicated agents at the concentrations recommended by Saito *et al.* (25). To examine the expression levels of NFBD1, we have generated a specific polyclonal antibody against the NH₂-terminal region of human NFBD1 (amino acid residues 1–150). The specificity of this antibody was verified by immunoblotting (data not shown). As shown in Fig. 1A, A549 cells treated with the indicated genotoxic agents underwent apoptosis in a dose-dependent manner as examined by MTT assay. Similar results were also obtained by fluorescence-activated cell sorter analysis (data not shown). In contrast, the nongenotoxic agents had undetectable effect on the viability of A549 cells. Immunoblot analysis revealed that the ADR treatment results in an accumulation of p53 as well as a phosphorylation of p53 at Ser-15, which is associated with a significant induction of one of the downstream effectors of p53, p21^{WAF1} (Fig. 1B). It is worth noting that NFBD1 is strongly reduced in response to ADR in a time-dependent manner. Similar results were also obtained in A549 cells exposed to CPT-11, CDDP, or VP-16. On the other hand, NFBD1 levels remained unchanged even at the later time points after the addition of NOX or PTX. Additionally, the treatment of A549 cells with these nongenotoxic agents had a marginal effect on the accumulation of p53 and p21^{WAF1} as compared with those of the genotoxic agents. Next, we performed RT-PCR using total RNA prepared from A549 cells exposed to 600 nM ADR for the indicated time periods. As shown in Fig. 1C, *NFBD1* mRNA levels were dramatically decreased in a time-dependent manner, accompanied with an up-regulation of *p21^{WAF1}*, *BAX*, *PUMA*, and *NOXA*. The expression levels of *p53* mRNA remained constant in ADR-treated A549 cells. These results suggest that NFBD1 is regulated at mRNA level in response to ADR.

Previously, it has been shown that NFBD1 associates with the members of the MRN complex, such as MRE11 and NBS1, and accumulates at nuclear foci in response to DNA damage (12, 14). Consistent with these observations, our immunofluorescence staining showed that NFBD1 co-localizes with NBS1 at nuclear foci within 1 h of exposing A549 cells to ADR, and NFBD1 nuclear foci are still present up to 24 h later (data not

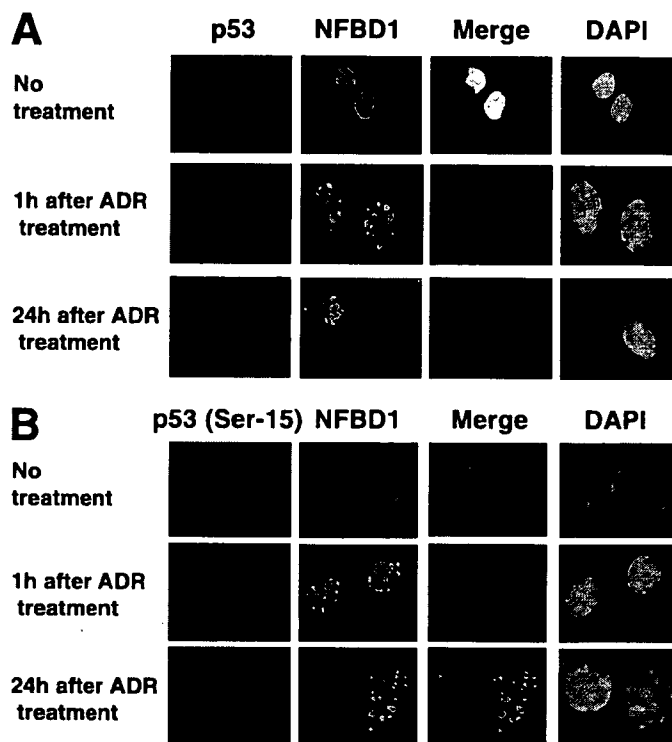


FIGURE 2. Subnuclear localization of NFBD1 and p53 in response to ADR. A and B, A549 cells were left untreated or treated with 600 nM ADR for the indicated time periods followed by incubation with the anti-NFBD1 and the anti-p53 antibodies (A), or with the anti-NFBD1 and anti-p53 (Ser-15) antibodies (B). Cell nuclei were stained with DAPI.

shown). ADR-mediated induction of p53 was undetectable after 1 h of treatment (Fig. 2A). Intriguingly, a significant nuclear accumulation as well as phosphorylation of p53 at Ser-15 was observed in cells 24 h after the treatment with ADR, which was associated with a disappearance of NFBD1 (Fig. 2, A and B). In contrast, NFBD1-containing nuclear foci were clearly present in cells lacking p53 induction. Collectively, these observations strongly suggest that there exists an inverse relationship between the expression of NFBD1 and p53 in response to DNA damage.

ADR-mediated Apoptosis in A549 Cells Is Regulated in a p53-dependent Manner—Because A549 cells carry wild-type *p53* (25), it is likely that the ADR-mediated apoptosis is regulated in a p53-dependent manner. To confirm this notion, we performed siRNA-mediated knockdown of p53. We transfected the empty plasmid or the expression plasmid for siRNA against p53 into A549 cells, and we established two control transfectants (C1 and C2) as well as two stable transfectants expressing siRNA for p53 (53R1 and 53R2) (Fig. 3A). We then performed MTT assay to examine a possible effect of p53 on the ADR-mediated apoptosis. As shown in Fig. 3B, 53R1 and 53R2 cells displayed a significant increase in cell viability as compared with the control transfectants and the parental A549 cells. Thus, it is likely that the ADR-mediated apoptosis in A549 cells is regulated at least in part in a p53-dependent manner.

To examine the possible effect of NFBD1 on the ADR-mediated apoptosis, A549 cells were transiently transfected with the empty plasmid or with the expression plasmid for NFBD1. Twenty four hours after transfection, cells were treated with

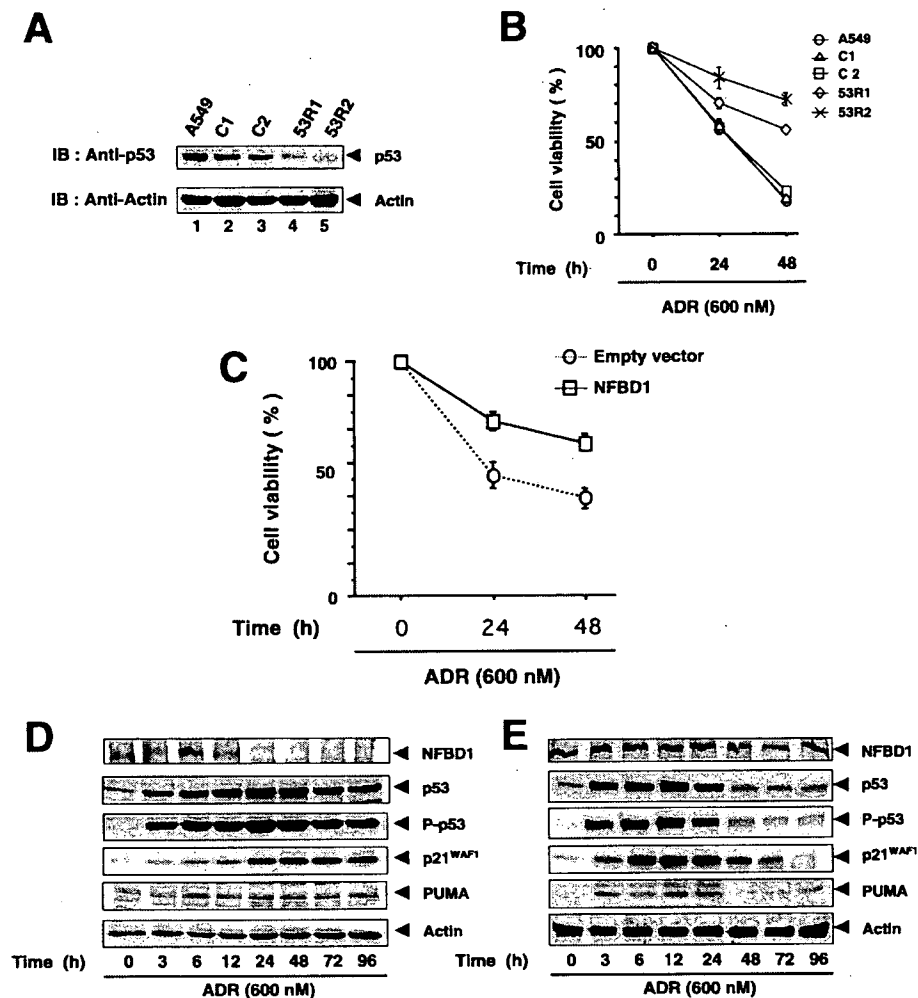


FIGURE 3. ADR-mediated apoptosis in A549 cells is regulated in a p53-dependent manner. *A*, knockdown of the endogenous p53. Whole cell lysates prepared from A549 cells stably expressing siRNA against p53 (53R1 and 53R2) or vector controls (C1 and C2) were processed for immunoblotting (IB) with the anti-p53 antibody (upper panel). Whole cell lysates were also analyzed for actin as a control for protein loading and nonspecific RNA interference effects (lower panel). *B*, cell survival assay. Parental A549 (open circle), C1 (open triangle), C2 (open square), 53R1 (open diamond), and 53R2 cells (cross) were exposed to 600 nM ADR. At the indicated time periods after the treatment with ADR, their cell survivals were examined by MTT assay. *C*, cell survival assay. A549 cells were seeded in 6-well plates at a density of 1×10^5 cells/well and transiently transfected with 1 μ g of the empty plasmid or with the NFBD1 expression plasmid. Twenty four hours after transfection, cells were exposed to 600 nM ADR. At the indicated time periods after the treatment with ADR, cell viability was examined by MTT assay. *D* and *E*, time course of the expression of p53 in response to ADR. A549 cells were transiently transfected with 2 μ g of the empty plasmid (*D*) or with the expression plasmid for NFBD1 (*E*). Twenty four hours after transfection, cells were treated with 600 nM ADR. At the indicated time periods after the treatment with ADR, whole cell lysates were prepared and processed for immunoblotting with the indicated antibodies.

600 nM ADR. At the indicated time periods after the addition of ADR, cell viability was measured by MTT assay. As shown in Fig. 3C, the enforced expression of NFBD1 caused a remarkable increase in cell viability as compared with that of cells transfected with the empty plasmid. We next determined the time course of p53 expression in A549 cells overexpressing NFBD1 in response to ADR. As shown in Fig. 3D, ADR-mediated accumulation as well as phosphorylation of p53 at Ser-15 became detectable as early as 3 h of ADR exposure, and the levels of p53 were maintained up to 96 h in control cells. In addition, p53-dependent induction of p21^{WAF1} and PUMA was detected at 6 h after the ADR treatment, and their expression levels persisted thereafter. In contrast, a significant reduction in the amounts and phosphorylation levels of p53 was detected in NFBD1-overexpressing cells at 24 h after the addition of ADR

with the empty plasmid. As expected, p53-mediated decrease in cell viability was restored by co-expression with NFBD1.

Effect of NFBD1 on the ADR-mediated Apoptosis—Next, we sought to examine the possible effect of the endogenous NFBD1 on the ADR-mediated apoptosis. To this end, we utilized an siRNA-mediated knockdown of NFBD1 in A549 cells as shown in Fig. 5A. Silencing of NFBD1 in A549 cells resulted in an increased sensitivity to ADR as compared with the control cells (Fig. 5B). To confirm the anti-apoptotic effect of NFBD1 in detail, A549 cells were transiently co-transfected with the constant amount of the GFP expression plasmid together with the empty plasmid, or with the expression plasmid for NFBD1 or siRNA against NFBD1. GFP served as an indicator for transfected cells. Twenty four hours after transfection, cells were treated with 600 nM ADR or left untreated and incubated for

(Fig. 3E). This down-regulation of p53 was associated with a decrease in the expression levels of p21^{WAF1} and PUMA. These results indicate that NFBD1 could inhibit the p53 phosphorylation at Ser-15, thereby reducing its transcriptional activity as well as stability.

NFBD1 Inhibits the p53-mediated Transcriptional Activation—To examine whether NFBD1 could affect the p53-mediated transcriptional activation, p53-deficient H1299 cells were transiently co-transfected with a constant amount of the expression plasmid for p53, luciferase reporter construct driven by the p53-responsive element derived from p21^{WAF1}, MDM2, or BAX promoter together with or without the increasing amounts of the NFBD1 expression plasmid, and luciferase activity was measured 48 h after transfection. As shown in Fig. 4, A–C, co-expression of p53 with NFBD1 resulted in a significant repression of the p53-mediated transcriptional activation. Consistent with the luciferase reporter assay, RT-PCR analysis revealed that NFBD1 inhibits the p53-mediated up-regulation of PUMA and BAX mRNA expression (Fig. 4D). To examine whether NFBD1 could affect the pro-apoptotic activity of p53, H1299 cells were transiently co-transfected with the indicated combinations of the expression plasmids, and their viability was measured by MTT assay. As shown in Fig. 4E, the enforced expression of p53 alone led to a decrease in cell viability as compared with that of cells transfected

Functional Interaction between NFBD1/MDC1 and p53

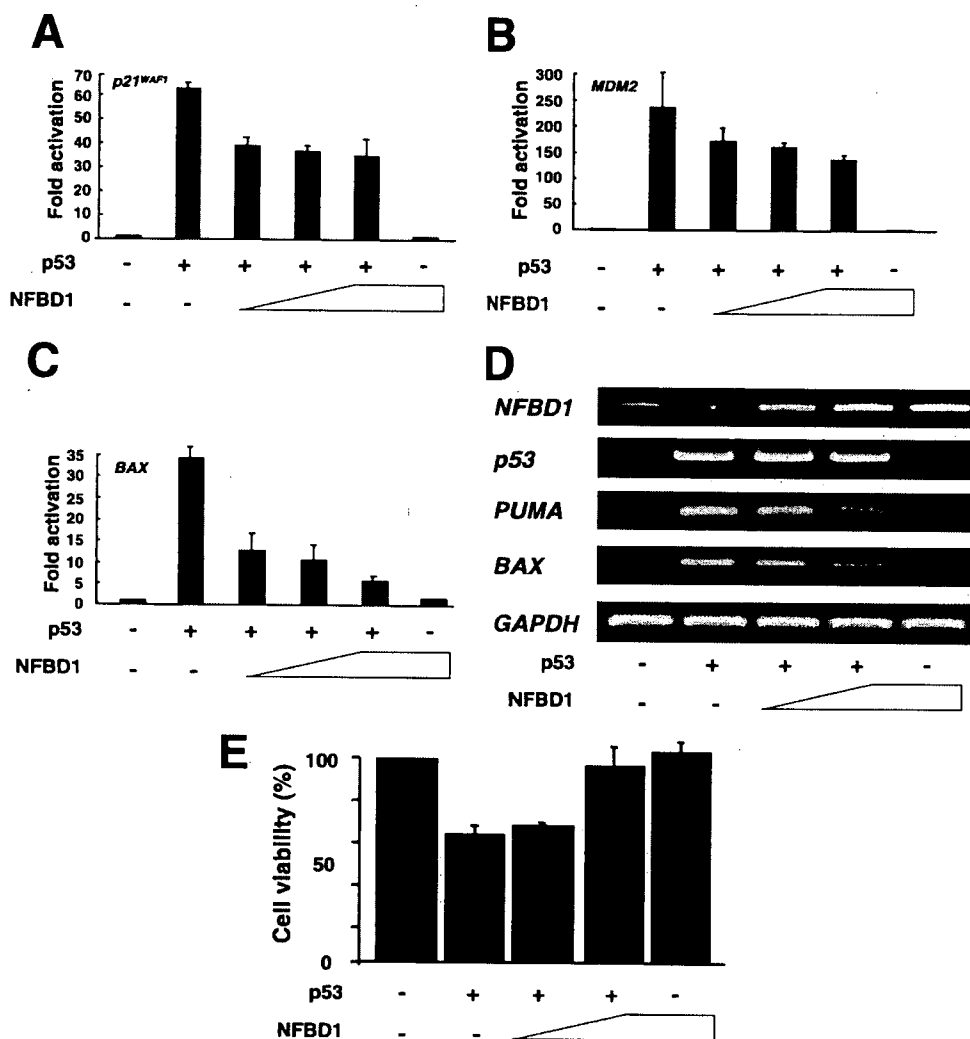


FIGURE 4. NFBD1 inhibits the transcriptional activity as well as pro-apoptotic function of p53. A–C, luciferase reporter analysis. H1299 cells were seeded in 12-well plates at a density of 5×10^4 cells/well. Cells were transiently co-transfected with 100 ng of the luciferase reporter construct carrying p53-responsive *p21^{WAF1}* (A), *MDM2* (B), or *BAX* (C) promoter, 10 ng of pRL-TK *Renilla* luciferase cDNA, and 25 ng of the expression plasmid for p53 together with or without the increasing amounts of the NFBD1 expression plasmid (25, 50, and 100 ng). Following 48 h of incubation, luciferase activity was measured and normalized for transfection efficiency using *Renilla* luciferase activity. The results were obtained from at least three sets of transfection and were presented as the mean \pm S.D. D, RT-PCR analysis. H1299 cells were transiently co-transfected with the constant amount of the expression plasmid for p53 (100 ng) together with or without the increasing amounts of the NFBD1 expression plasmid (400 and 800 ng). Twenty four hours after transfection, total RNA was prepared and analyzed by RT-PCR for the expression levels of *NFBD1*, *p53*, *PUMA*, and *BAX*. The expression level of *GAPDH* was measured as an internal control. E, cell survival assay. The constant amount of the p53 expression plasmid (200 ng) was transiently co-transfected into H1299 cells together with or without the increasing amounts of the NFBD1 expression plasmid (400 and 800 ng). Total amount of DNA was kept constant (1 μ g) with the empty plasmid. Forty eight hours later, cell viability was examined by MTT assay.

another 24 h. Cell nuclei were then stained with DAPI, and the number of GFP-positive cells with apoptotic nuclei was scored. The enforced expression of NFBD1 led to a decrease in the number of apoptotic cells in response to ADR as compared with that of the control cells (Fig. 5, C and D). As expected, siRNA-mediated knockdown of NFBD1 caused a significant increase in the number of apoptotic cells in response to ADR. In contrast to A549 cells, overexpression of NFBD1 and silencing of NFBD1 in p53-deficient H1299 cells had an undetectable effect on the ADR-mediated apoptosis (Fig. 5E). Taken together, these results strongly suggest that NFBD1 prevents the ADR-mediated apoptosis by modulating p53.

Next, we examined the possible effect of the siRNA-mediated knockdown of the endogenous NFBD1 on the p53-mediated transcriptional activation. For this purpose, H1299 cells were transiently co-transfected with the constant amount of p53 expression plasmid together with or without the increasing amounts of the expression plasmid for siRNA against NFBD1. As shown in Fig. 6, A–C, siRNA-mediated knockdown of the endogenous NFBD1 in H1299 cells increased the p53-dependent luciferase activities driven from *p21^{WAF1}*, *MDM2*, or *BAX* promoter. In addition, similar results were obtained in U2OS cells bearing wild-type p53 (supplemental Fig. 1). Furthermore, the down-regulation of the endogenous NFBD1 resulted in a significant increase in the phosphorylation levels of p53 at Ser-15 as well as the amount of p53 (Fig. 6D). Under our experimental conditions, the exogenously expressed p53 was phosphorylated in the absence of DNA-damaging agents. Similar observations were also described (26). These results strongly suggest that NFBD1 inhibits the transcriptional as well as pro-apoptotic activity of p53 through the down-regulation of p53.

Physical Interaction between NFBD1 and p53—To examine whether NFBD1 could interact with p53 in cells, whole cell lysates prepared from HEK293T cells were immunoprecipitated with NRS or with the polyclonal anti-NFBD1 antibody, and the immunoprecipitates were analyzed by immunoblotting with the monoclonal anti-p53 antibody. As shown Fig. 7A, the anti-NFBD1 immunoprecipitates contained the endogenous p53, suggesting that NFBD1 forms a complex with p53. Similarly, the anti-p53 immunoprecipitates contained the endogenous NFBD1. To map the region(s) of p53 required for the interaction with NFBD1, H1299 cells were transiently co-transfected with the expression plasmid for NFBD1 together with the expression plasmid for p53-(1–359), p53-(1–292), p53-(1–101), or with p53-(102–393) (Fig. 7B). Forty eight hours after transfection, whole cell lysates were prepared and processed for the immunoprecipitation with the indicated antibodies. As shown in Fig. 7, C–F, all of the p53 deletion mutants except p53-(102–393) retained an ability to interact with NFBD1,

Functional Interaction between NFB1/MDC1 and p53

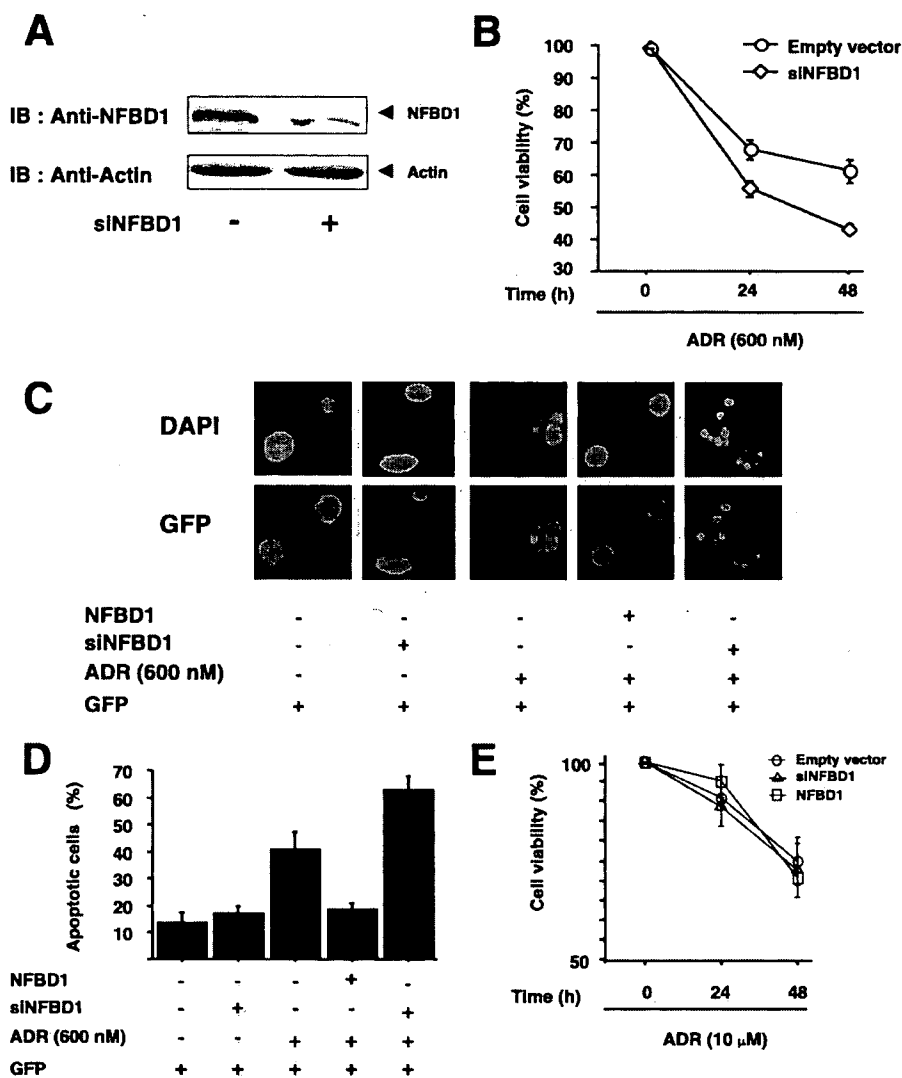


FIGURE 5. siRNA-mediated down-regulation of the endogenous NFB1 promotes the ADR-dependent apoptosis. *A*, reduction of the endogenous NFB1 by siRNA against NFB1. A549 cells were transiently transfected with the expression plasmid for siRNA against NFB1 termed siNFB1 or with the empty plasmid. Forty eight hours after transfection, whole cell lysates were analyzed for the expression level of the endogenous NFB1 by immunoblotting (IB) and also analyzed for actin as a control for protein loading and nonspecific RNA interference effects. *B*, cell survival assay. A549 cells were transiently transfected with the empty plasmid (open circle) or with NFB1-siRNA (open diamond). Twenty four hours post-transfection, cells were treated with 600 nM ADR. At the indicated time periods after the treatment with ADR, cell viability was measured by MTT assay. *C* and *D*, apoptosis assay. A549 cells were transiently co-transfected with the constant amount of the expression plasmid for GFP together with or without the NFB1 expression plasmid or siNFB1. Twenty four hours after transfection, cells were treated with ADR (600 nM) for another 24 h. Cell nuclei were stained with DAPI, and transfected cells were identified by the presence of green fluorescence (*C*). The number of GFP-positive cells with apoptotic nuclei was scored (*D*). *E*, NFB1 has undetectable effect on the ADR-induced apoptosis in p53-deficient H1299 cells. H1299 cells were transfected with the empty plasmid (open circle), expression plasmid for NFB1 (open square), or siNFB1 (open triangle). Twenty four hours after transfection, cells were exposed to 10 μM ADR for 24, 48, and 72 h, and their viability was then examined as described in *B*.

suggesting that the NH₂-terminal region of p53 is required for the interaction with NFB1.

Phosphorylated Forms of p53 Do Not Bind to NFB1—Our preliminary experiments indicated that λ-phosphatase treatment of ADR-treated whole cell lysates significantly increases an ability of BRCT domain of NFB1 (see below) to interact with endogenous p53 (data not shown). These results prompted us to examine whether the phosphorylation of p53 could affect the interaction with NFB1. As shown in Fig. 8, the detailed analysis of the time course of NFB1/p53 interaction in A549 cells in response to ADR demonstrated that p53 phos-

phorylated at Ser-15 fails to be co-immunoprecipitated with NFB1 during the ADR-mediated apoptosis. In addition, the NFB1-p53 complex was detected in untreated cells and remained at high levels for 3 h of the ADR treatment, after which the amounts of this complex slowly decreased.

BRCT Domain of NFB1 Is Required for the Interaction with p53—We sought to determine the essential region(s) of NFB1 required for the interaction with p53. To this end, we generated the expression plasmids for FLAG-FHA, FLAG-PST, and FLAG-BRCT (Fig. 9A). To examine the subcellular distribution of the NFB1 deletion mutants, COS7 cells were transiently transfected with these expression plasmids. Forty eight hours after transfection, cells were fractionated into nuclear and cytoplasmic fractions and subjected to immunoblotting. As shown in Fig. 9B, FLAG-PST and FLAG-BRCT were expressed in both the nucleus and cytoplasm, whereas FLAG-FHA was detected in the cytoplasm. Because of the different subcellular distribution of the NFB1 deletion mutants, we performed the *in vitro* pulldown assays. Whole cell lysates prepared from COS7 cells were incubated with the radiolabeled NFB1 deletion mutants and then immunoprecipitated with the anti-p53 antibody. The anti-p53 immunoprecipitates were analyzed by SDS-PAGE followed by autoradiography. As shown in Fig. 9C, the BRCT domains were required for the maximal binding to p53.

The BRCT Domains of NFB1 Have an Ability to Down-regulate p53—To investigate the functional

significance of the BRCT domains of NFB1 in the regulation of p53, A549 cells were transiently transfected with or without the increasing amounts of the expression plasmid for FLAG-BRCT. Twenty four hours after transfection, cells were exposed to ADR and incubated for another 24 h. Whole cell lysates were then prepared and subjected to immunoblotting with the indicated antibodies. FLAG-FHA was used as a negative control. As shown in Fig. 10A, the ADR-mediated accumulation and phosphorylation of p53 at Ser-15 were inhibited by FLAG-BRCT. This down-regulation of p53 was associated with a decrease in the expression levels of BAX and p21^{WAF1}. In contrast, FLAG-

Functional Interaction between NFBD1/MDC1 and p53

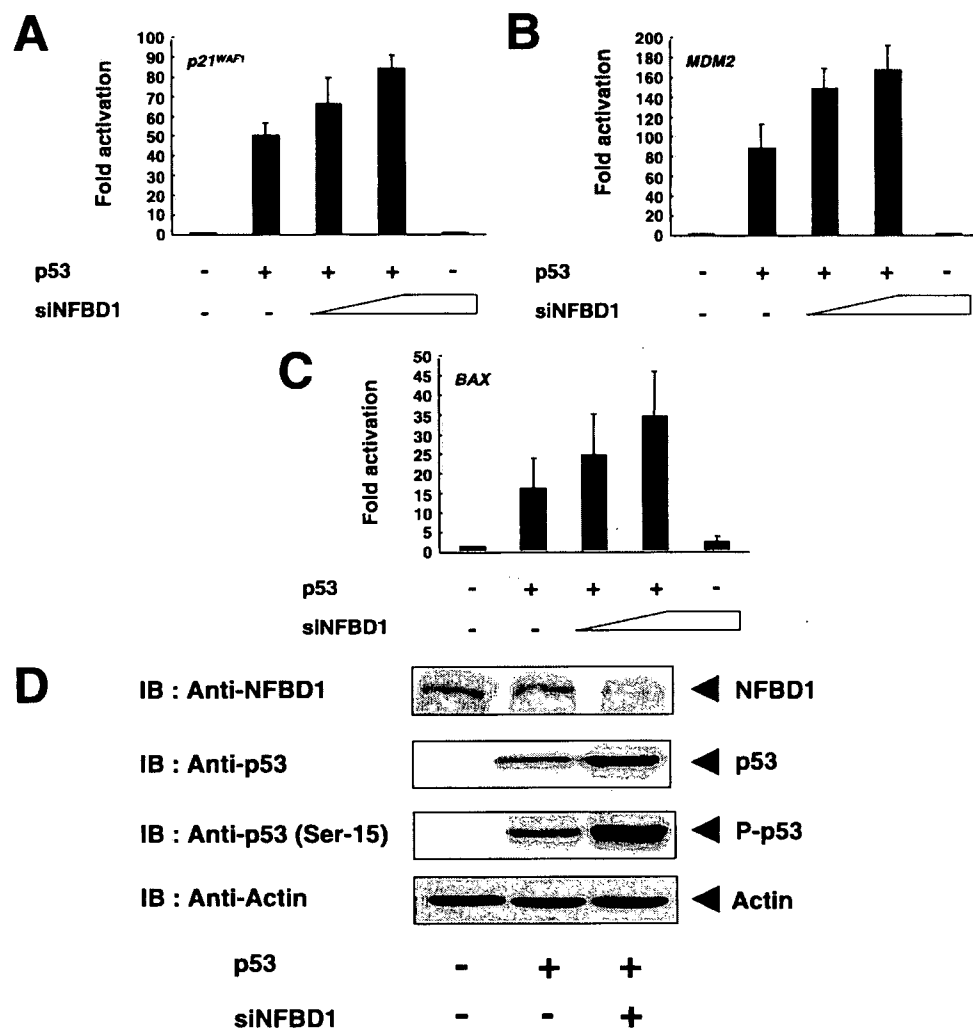


FIGURE 6. siRNA-mediated knockdown of NFBD1 enhances the p53-dependent transcriptional activation. A–C, luciferase reporter analysis. H1299 cells were transiently co-transfected with the constant amount of the expression plasmid for p53, luciferase reporter construct driven by the p53-responsive element derived from *p21^{WAF1}* (A), *MDM2* (B), or *BAX* (C) promoter, and pRL-TK *Renilla* luciferase cDNA together with or without the increasing amounts of the expression plasmid for siRNA against NFBD1. Forty eight hours after transfection, cell lysates were prepared, and luciferase activity was measured. D, siRNA-mediated knockdown of NFBD1 increases the phosphorylation of p53 at Ser-15. H1299 cells were transiently co-transfected with the constant amount of the expression plasmid for p53 together with or without the expression plasmid encoding siRNA against NFBD1. Whole cell lysates were examined by immunoblotting (IB) with the indicated antibodies.

FHA, which was localized exclusively in cytoplasm, had no significant effect on p53 (Fig. 10B). Thus, it is likely that the BRCT domains of NFBD1 play a crucial role not only in the physical interaction with p53 but also in the down-regulation of p53.

DISCUSSION

A growing body of evidence strongly suggests that NFBD1 mediates the rapid recruitment of the MRN complex into the sites of DNA damage, and thus facilitates the efficient repair of DNA double strand breaks before the cells undergo DNA replication (27). NFBD1 also has an anti-apoptotic function in response to DNA damage. For example, siRNA-mediated depletion of the endogenous NFBD1 resulted in the increased sensitivity to irradiation and anti-cancer drug (13–16). Recently, it has been shown that NFBD1-deficient mice display the abnormal phenotypes, including chromosome instability, DNA repair defects, and radiation sensitivity (28). However,

the detailed molecular mechanism behind the anti-apoptotic effect of NFBD1 is still largely elusive. In this study, we have found that NFBD1 interacts with tumor suppressor p53, reduces its phosphorylation at Ser-15 in response to ADR, and thereby inhibiting the transcriptional as well as pro-apoptotic activity of p53. Thus, our present findings would help to shed light on the currently unknown molecular mechanisms underlying the NFBD1-mediated anti-apoptotic effect in response to DNA damage.

During the DNA damage-induced apoptosis, p53 is activated by a complex series of phosphorylations within its NH₂-terminal transactivation domain (reviewed in Ref. 24). The catalytic activity of ATM is markedly increased in response to DNA damage and is responsible for the rapid phosphorylation of p53 at Ser-15, as described previously (20, 21). This ATM-mediated phosphorylation contributes to the enhanced activity as well as stability of p53 by facilitating its dissociation from E3 ubiquitin protein ligase MDM2 (29). When Ser-15 was replaced by Ala, the transcriptional activity of p53 was significantly reduced (30). Under our experimental conditions, ADR treatment induced p53 accumulation and phosphorylation at Ser-15 in A549 cells. Recently, Peng and Chen (31) reported that 53BP1 and NFBD1 are required for the recruitment of ATM-Rad3-related into the DNA

damage sites, suggesting that ATM-Rad3-related as well as ATM might also participate in this process. On the other hand, little increase in phosphorylation at Ser-20 as well as Ser-46 in response to ADR was observed at any time examined (data not shown). It is worth noting that the ADR-induced phosphorylation of p53 at Ser-15 was associated with a strong down-regulation of NFBD1, and the high p53 phosphorylation levels persisted even 96 h after the treatment. Constitutive expression of NFBD1 resulted in a remarkable decrease in the phosphorylation levels of p53 at Ser-15 24–48 h after the ADR treatment. Consistent with these results, the siRNA-mediated knockdown of the endogenous NFBD1 in H1299 cells led to a significant phosphorylation of the exogenous p53 at Ser-15, indicating that NFBD1 has an inhibitory role in the regulation of p53. This notion was further supported by the facts that the p53-mediated transcriptional activation and apoptosis are impaired by NFBD1.

Functional Interaction between NFBD1/MDC1 and p53

Based on our immunoprecipitation experiments, NFBD1 bound to the NH₂-terminal region of p53, including its transactivation domain. MDM2 attenuates the transcriptional activity of p53 by binding to and masking its transactivation domain, as described previously (32). MDM2 also acts as an E3 ubiquitin protein ligase for p53 and promotes its ubiquitination-dependent

proteasomal turnover. It has been shown that Ser-15 phosphorylation impairs the interaction between p53 and MDM2 and leads to the subsequent stabilization and activation of p53 (29). Phosphorylation at Ser-15 also stimulates p53 interaction with its transcriptional co-activators such as p300/CBP (30, 33). Alternatively, tumor suppressor p19^{ARF} directly interacts with

MDM2 to inhibit its E3 ubiquitin protein ligase activity, thereby preventing the MDM2-mediated degradation of p53 (34–37). In addition, Maya *et al.* (38) reported that MDM2 is phosphorylated by ATM in response to DNA damage, and this phosphorylation attenuates its inhibitory potential on p53. Our preliminary results indicated that NFBD1 is associated with MDM2 as examined by co-immunoprecipitation assay (data not shown). Considering that NFBD1 directly interacts with the NH₂-terminal region of p53, it is likely that NFBD1 might mask the Ser-15 to prevent its phosphorylation mediated by ATM, and/or recruit MDM2 to the NH₂-terminal region of p53 to facilitate MDM2-mediated proteolytic degradation of p53. Further studies will be necessary to clarify this issue.

NFBD1 contains several protein-protein interaction domains. Xu and Stern (15) demonstrated that NFBD1-derived FHA and BRCT domains are necessary for the interaction with MRN complex and γ H2AX, respectively. According to our *in vitro* binding analysis, NFBD1 bound to p53 mainly through its BRCT domains. Consistent with these results, BRCT domains of NFBD1 retained an abil-

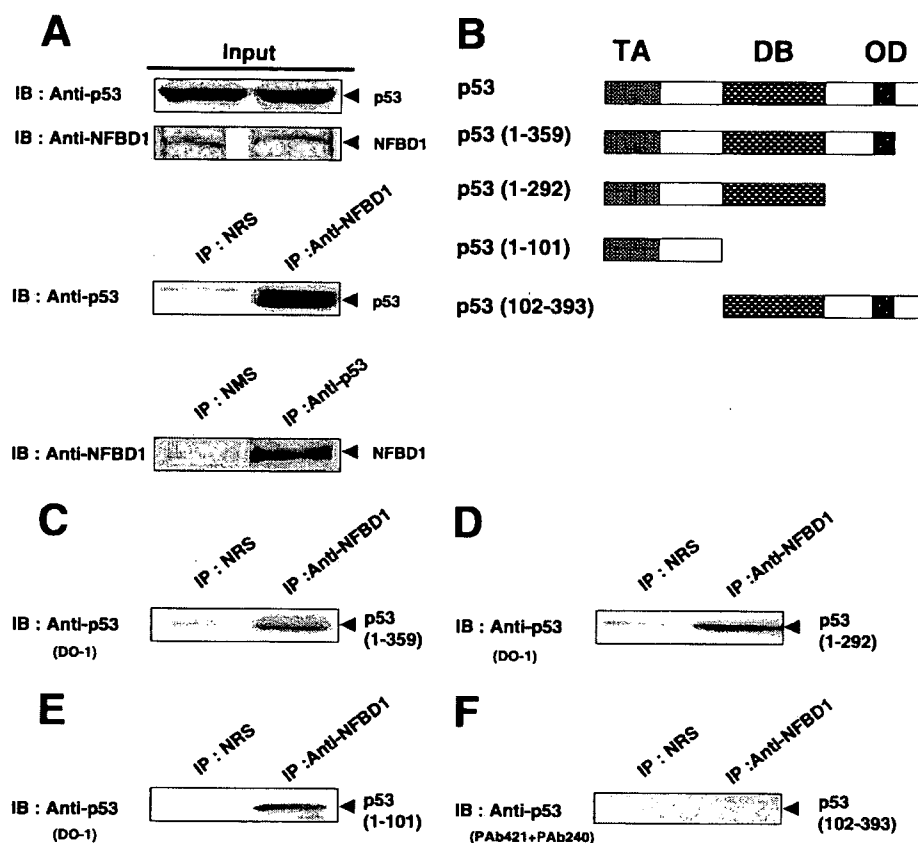


FIGURE 7. Interaction between NFBD1 and p53 in cells. A, immunoprecipitation. Whole cell lysates prepared from HEK293T cells were immunoprecipitated (IP) with NRS or with the polyclonal anti-NFBD1 antibody, or immunoprecipitated with normal mouse serum (NMS) or with monoclonal anti-p53 antibody, and the immunoprecipitates were analyzed by immunoblotting (IB) with the monoclonal anti-p53 or with polyclonal anti-NFBD1 antibody, respectively. B, schematic drawing of the full-length p53 and various p53 deletion mutants used in this study. TA, transactivation domain; DB, DNA-binding domain; OD, oligomerization domain. C–F, NFBD1 interacts with the NH₂-terminal region of p53 containing its transactivation domain. H1299 cells were transiently co-transfected with the indicated combinations of the expression plasmids. Forty eight hours after transfection, whole cell lysates were prepared and subjected to immunoprecipitation with NRS or with the polyclonal anti-NFBD1 antibody followed by immunoblotting with the indicated anti-p53 antibodies.

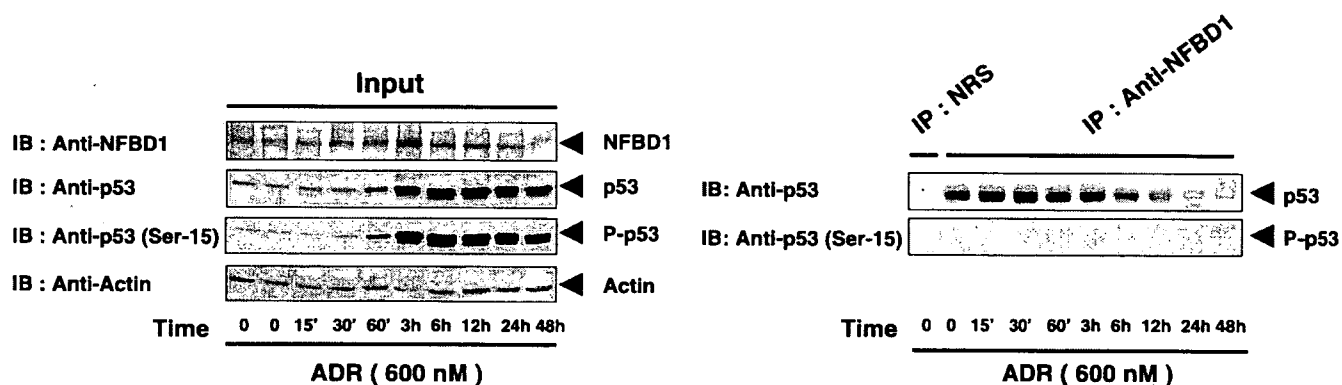


FIGURE 8. p53 phosphorylated at Ser-15 does not interact with NFBD1 in cells. A549 cells were exposed to 600 nM ADR. At the indicated time points after the treatment with ADR, whole cell lysates were prepared and immunoprecipitated (IP) with NRS or with the anti-NFBD1 antibody followed by immunoblotting (IB) with the anti-p53 or with the anti-p53 (Ser-15) antibody (right panel). Input amounts of proteins were determined by immunoblotting with the indicated antibodies (left panel). Actin was used as a loading control.

Functional Interaction between NFBD1/MDC1 and p53

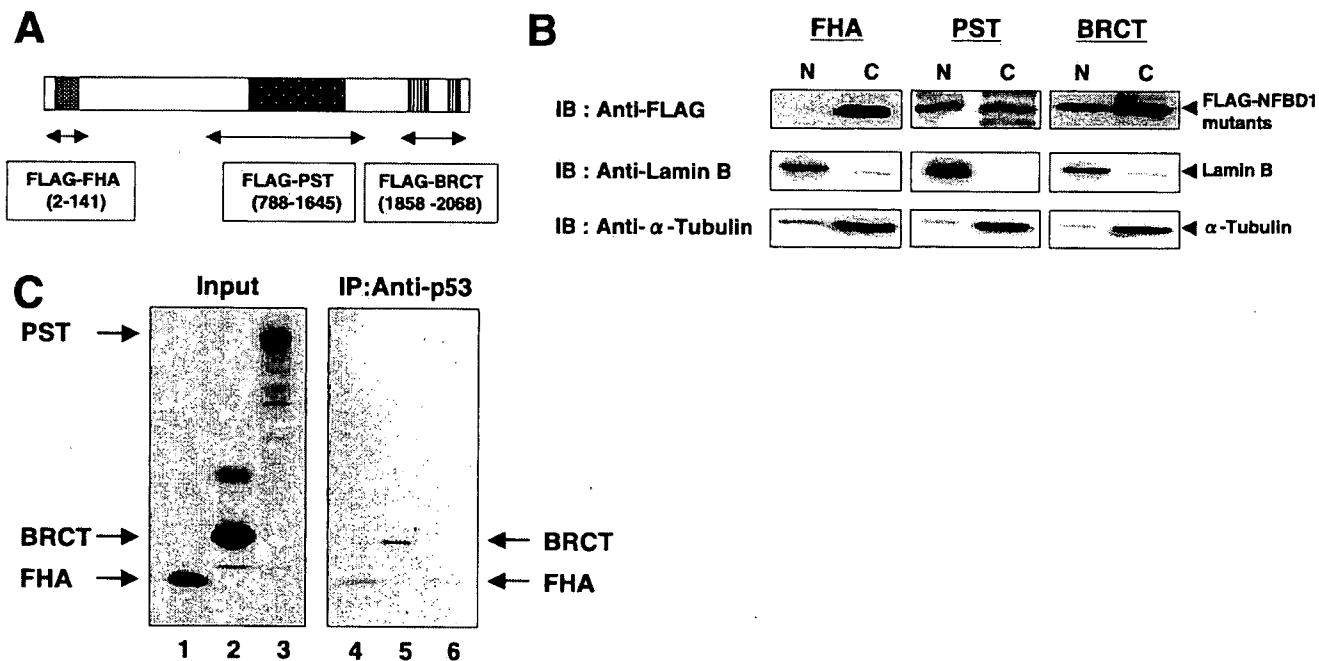


FIGURE 9. BRCT domains of NFBD1 are required for the interaction with p53. *A*, schematic representation of FLAG-NFBD1 mutants. *Number* indicates amino acid position. *B*, subcellular localization of NFBD1 mutants. COS7 cells were transiently transfected with the indicated expression plasmids. Forty eight hours after transfection, cells were fractionated into nuclear (*N*) and cytoplasmic (*C*) fractions. Equal amounts of each fraction were separated by 10% SDS-PAGE and immunoblotted (*IB*) with the anti-FLAG antibody (*top panel*). Samples were also immunoblotted with the antibody specific for lamin B (*middle panel*) or with the anti- α -tubulin (*bottom panel*) to show the purity of each fraction. *C*, *in vitro* binding assay. Whole cell lysates prepared from COS7 cells were incubated with the radiolabeled FLAG-FHA, FLAG-BRCT, or with FLAG-PST and immunoprecipitated (*IP*) with the anti-p53 antibody. Immunoprecipitates were separated by 10% SDS-PAGE, and the radiolabeled bound proteins were visualized by autoradiography.

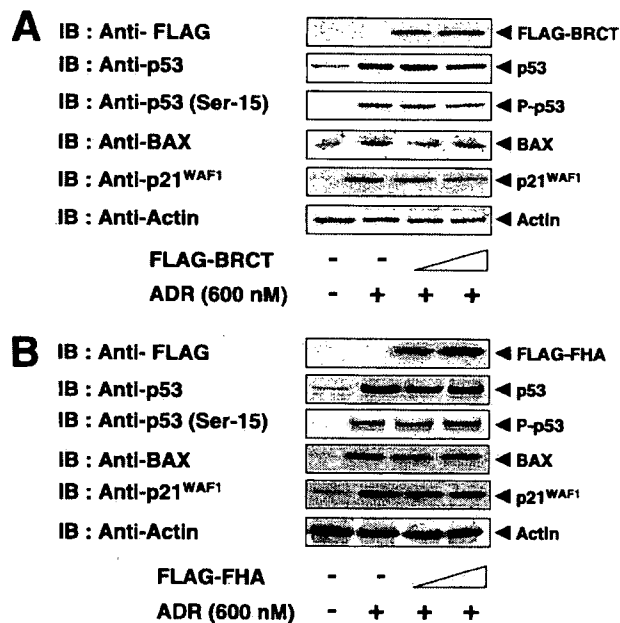


FIGURE 10. BRCT domains of NFBD1 retain an ability to inhibit the induction of p53 in response to ADR. *A* and *B*, immunoblot (*IB*) analysis. A549 cells were transiently transfected with the increasing amounts of the FLAG-BRCT (*A*) or with the FLAG-FHA expression plasmid (*B*). The total amount of DNA was kept constant (2 μ g) with pcDNA3. Twenty four hours after transfection, cells were left untreated or treated with 600 nM ADR and incubated for another 24 h. Whole cell lysates were then prepared and analyzed by immunoblotting with the indicated antibodies.

ity to reduce the p53 phosphorylation levels at Ser-15 as well as to decrease the stability of p53. In contrast, the FHA domain-containing fragment had no significant effect on p53 because of its cytoplasmic localization. BRCT domains mediate phospho-

rylation-dependent protein-protein interaction, as described previously (39–41). For example, the BRCT domains of BRCA1 recognize specific phospho-Ser-containing peptides (40). In contrast, unphosphorylated forms of p53 bound to the BRCT domains of NFBD1 much more efficiently *in vitro* relative to phosphorylated forms of p53 (data not shown). Furthermore, NFBD1 failed to bring down p53 phosphorylated at Ser-15 as examined by co-immunoprecipitation experiments. Thus, it is likely that BRCT domains of NFBD1 do not always prefer phospho-Ser-containing peptides.

It has been shown that NFBD1 cooperates with the histone variant H2AX to recruit DNA repair proteins such as MRN complex to the sites of DNA damage (27). In accordance with this notion, NFBD1 displayed diffuse nuclear staining under normal conditions, whereas NFBD1 redistributed to nuclear foci within 1 h after the treatment with ADR. The NFBD1 nuclear foci co-localized with NBS1 and lasted at least 24 h after the ADR treatment (data not shown). The ADR-induced accumulation of p53 was not clearly detected within 1 h of exposure. At a single cell level, the ADR-induced NFBD1 nuclear foci were present only in cells lacking p53 accumulation and phosphorylation at Ser-15 24 h after the treatment. In contrast, NFBD1 nuclear foci were undetectable in cells expressing p53. These observations were consistent with the inverse relationship between the expression levels of p53 and NFBD1 in response to ADR. Considering that NFBD1 directly interacts with p53, thereby preventing its phosphorylation at Ser-15, it is possible that NFBD1 participates in the early cellular responses to ADR, and the ADR-induced down-regulation of NFBD1 might be crucial for the initiation of the p53-dependent apoptotic response.

Expression analysis showed that NFBD1 is regulated at mRNA level in response to ADR. To explore the molecular mechanisms regulating the p53-mediated DNA damage signaling pathways, it is necessary to identify the promoter region as well as the transcription factor(s) responsible for the regulation of NFBD1 upon treatment with ADR. Although the transcriptional regulatory mechanism of NFBD1 has remained elusive, the extensive search of the human genomic sequence information revealed that there exists a putative NF- κ B-binding site within the intron 3 of the *NFBD1* gene (data not shown). Accumulating evidence suggests that NF- κ B plays an important role in cellular protection against a wide variety of apoptotic stresses, including DNA damage (42–45). For example, camptothecin-mediated activation of NF- κ B was transient, and the impaired activation of NF- κ B resulted in an enhanced sensitivity to camptothecin (46). Similar results were also obtained in cells exposed to ADR (47). Furthermore, the recent study indicated that ATM is required for NF- κ B activation in response to DNA damage (48, 49), and NF- κ B activation decreases the stability of p53, which might be due to the up-regulation of MDM2 (50). Collectively, it is possible that the transient activation of NF- κ B might maintain and/or induce the expression levels of NFBD1 and MDM2, which is required for cell survival following DNA damage. However, it remains to be clarified whether NF- κ B could regulate the expression of NFBD1 in response to DNA damage. Recently, Townsend *et al.* (51) described that *NFBD1* might be a direct transcriptional target of STAT-1. According to their results, the expression levels of NFBD1 were reduced in STAT-1-deficient cells but were restored by the exogenous expression of STAT-1. Under our experimental conditions, however, we could not detect the STAT-1-mediated transcriptional up-regulation of *NFBD1* (data not shown). This discrepancy might be due to the cell type-specific effects. Thus, it is likely that there could exist a separate and distinct transcription factor(s) required for the transcriptional regulation of *NFBD1*. Studies to elucidate the molecular mechanisms of the transcriptional regulation of *NFBD1* in response to DNA damage are underway.

Acknowledgments—We thank Dr. T. Kamijo for helpful discussions. We also thank Y. Nakamura and S. Ono for excellent technical assistance.

REFERENCES

- Koonin, E. V., Altschul, S. F., and Bork, P. (1996) *Nat. Genet.* **13**, 266–267
- Bork, P., Hofmann, K., Bucher, P., Neuwald, A. F., Altschul, S. F., and Koonin, E. V. (1997) *FASEB J.* **11**, 68–76
- Callebaut, I., and Mornon, J. P. (1997) *FEBS Lett.* **400**, 25–30
- Chapman, M. S., and Verma, I. M. (1996) *Nature* **382**, 678–679
- Monteiro, A. N. A., August, A., and Hanafusa, H. (1996) *Proc. Natl. Acad. Sci. U. S. A.* **93**, 13595–13599
- Scully, R., Anderson, S. F., Chao, D. M., Wei, W., Ye, L., Young, R. A., Livingston, D. M., and Parvin, J. D. (1997) *Proc. Natl. Acad. Sci. U. S. A.* **94**, 5605–5610
- Bork, P., and Koonin, E. V. (1996) *Curr. Opin. Struct. Biol.* **6**, 366–376
- Iwabuchi, K., Bartel, P. L., Li, B., Marraccino, R., and Fields, S. (1994) *Proc. Natl. Acad. Sci. U. S. A.* **91**, 6098–6102
- Chai, Y. L., Cui, J., Shao, N., Shyam, E., Reddy, P., and Rao, V. N. (1999) *Oncogene* **18**, 263–268
- Nagase, T., Seki, N., Ishikawa, K., Tanaka, A., and Nomura, N. (1996) *DNA Res.* **3**, 17–24
- Ozaki, T., Nagase, T., Ichimiya, S., Seki, N., Ohira, M., Nomura, N., Takada, N., Sakiyama, S., Weber, B. L., and Nakagawara, A. (2000) *DNA Cell Biol.* **19**, 475–485
- Goldberg, M., Stucki, M., Falck, J., D'Amours, D., Rahman, D., Pappin, D., Jiri, B., and Jackson, S. P. (2003) *Nature* **421**, 952–956
- Lou, Z., Minter-Dykhouse, K., Wu, X., and Chen, J. (2003) *Nature* **421**, 957–961
- Stewart, G. S., Wang, B., Bignell, C. R., Taylor, A. M. R., and Elledge, S. J. (2003) *Nature* **421**, 961–966
- Xu, X., and Stern, D. F. (2003) *FASEB J.* **17**, 1842–1848
- Peng, A., and Chen, P. L. (2003) *J. Biol. Chem.* **278**, 8873–8876
- Xu, X., and Stern, D. F. (2003) *J. Biol. Chem.* **278**, 8795–8803
- Lou, Z., Chen, B. P.-C., Asaithamby, A., Minter-Dykhouse, K., Chen, D. J., and Chen, J. (2004) *J. Biol. Chem.* **279**, 46359–46362
- Shieh, S. Y., Ahn, J., Tamai, K., Taya, Y., and Prives, C. (2000) *Genes Dev.* **14**, 289–300
- Banin, S., Moyal, L., Shieh, S., Taya, Y., Anderson, C. W., Chessa, L., Smorodinsky, N. I., Prives, C., Reiss, Y., Shiloh, Y., and Ziv, Y. (1998) *Science* **281**, 1674–1677
- Canman, C. E., Lim, D. S., Cimprich, K. A., Taya, Y., Tamai, K., Sakaguchi, K., Appella, E., Kastan, M. B., and Siliciano, J. D. (1998) *Science* **281**, 1677–1679
- Chehab, N. H., Malikzay, A., Appel, M., and Halazonetis, T. D. (2000) *Genes Dev.* **14**, 278–288
- Hirao, A., Kong, Y. Y., Matsuoka, S., Wakeham, A., Ruland, J., Yoshida, H., Liu, D., Elledge, S. J., and Mak, T. W. (2000) *Science* **287**, 1824–1827
- Vousden, K. H. (2002) *Biochim. Biophys. Acta* **1602**, 47–59
- Saito, S., Yamaguchi, H., Higashimoto, Y., Chao, C., Xu, Y., Fornace, A., Jr., Appella, E., and Anderson, W. (2003) *J. Biol. Chem.* **278**, 37536–37544
- Rodicker, F., and Putzer, B. M. (2003) *Cancer Res.* **63**, 2737–2741
- Stucki, M., and Jackson, S. P. (2004) *DNA Repair* **3**, 953–957
- Lou, Z., Minter-Dykhouse, K., Franco, S., Gostissa, M., Rivera, M. A., Celeste, A., Manis, J. P., van Deursen, J., Nussenzweig, A., Alt, F. W., and Chen, J. (2006) *Mol. Cell* **21**, 187–200
- Shieh, S. Y., Ikeda, M., Taya, Y., and Prives, C. (1997) *Cell* **91**, 325–334
- Dumaz, N., and Meek, D. W. (1999) *EMBO J.* **18**, 7002–7010
- Peng, A., and Chen, P. L. (2005) *Cancer Res.* **65**, 1158–1163
- Freedman, D. A., Wu, L., and Levine, A. J. (1999) *Cell. Mol. Life Sci.* **55**, 96–107
- Lambert, P. F., Kashanchi, F., Radonovich, M. F., Shiekhatter, R., and Brady, J. N. (1998) *J. Biol. Chem.* **273**, 33048–33053
- Zhang, Y., Xiong, Y., and Yarbrough, W. G. (1998) *Cell* **92**, 725–734
- Pomerantz, J., Schreiber Agus, N., Liegeois, N. J., Silverman, A., Alland, L., Chin, L., Potes, J., Chen, K., Orlov, I., Lee, H. W., Cordon-Cardo, C., and DePinho, R. A. (1998) *Cell* **92**, 713–723
- Weber, J. D., Taylor, L. J., Roussel, M. F., Sherr, C. J., and Bar-Sagi, D. (1999) *Nat. Cell Biol.* **1**, 20–26
- Honda, R., and Yasuda, H. (1999) *EMBO J.* **18**, 22–27
- Maya, R., Balass, M., Kim, S. T., Shkedy, D., Leal, J. F., Shifman, O., Moas, M., Buschmann, T., Ronai, Z., Shiloh, Y., Kastan, M. B., Katzil, E., and Oren, M. (2001) *Genes Dev.* **15**, 1067–1077
- Manke, I. A., Lowery, D. M., Nguyen, A., and Yaffe, M. B. (2003) *Science* **302**, 636–639
- Rodriguez, M., Yu, X., Chen, J., and Songyang, Z. (2003) *J. Biol. Chem.* **278**, 52914–52918
- Yu, X., Chini, C. C., He, M., Mer, G., and Chen, J. (2003) *Science* **302**, 639–642
- Beg, A. A., and Baltimore, D. (1996) *Science* **274**, 782–784
- Liu, Z. G., Hsu, H., Goeddel, D. V., and Karin, M. (1996) *Cell* **87**, 565–576
- Van Antwerp, D. J., Martin, S. J., Kafri, T., Green, D. R., and Verma, I. M. (1996) *Science* **274**, 787–789
- Wang, C. Y., Mayo, M. W., and Baldwin, A. S. J. (1996) *Science* **274**, 784–787
- Huang, T. T., Wuertzberger-Davis, S. M., Seufzer, B. J., Shumway, S. D., Kimura, T., Boothman, D. A., and Miyamoto, S. (2000) *J. Biol. Chem.* **275**, 9501–9509
- Bian, X., McAllister-Lucas, L. M., Shao, F., Schumacher, K. R., Feng, Z.,

Functional Interaction between NFB1/MDC1 and p53

- Porter, G., Castle, V. P., and Opirari, A. W., Jr. (2001) *J. Biol. Chem.* **276**, 48921–48929
48. Li, N., Banin, S., Ouyang, H., Li, G. C., Courtois, G., Shiloh, Y., Karin, M., and Rotman, G. (2001) *J. Biol. Chem.* **276**, 8898–8903
49. Panta, G. R., Kaur, S., Cavin, L. G., Cortes, M. L., Mercurio, F., Lothstein, L., Sweatman, T. W., Israel, M., and Arsura, M. (2004) *Mol. Cell. Biol.* **24**, 1823–1835
50. Tergaonkar, V., Pando, M., Vafa, O., Wahl, G., and Verma, I. (2002) *Cancer Cell* **1**, 493–503
51. Townsend, P. A., Cragg, M. S., Davidson, S. M., McCormick, J., Barry, S., Lawrence, K. M., Knight, R. A., Hubank, M., Chen, P. L., Latchman, D. S., and Stephanou, A. (2005) *J. Cell Sci.* **118**, 1629–1639

3-Methyladenine suppresses cell migration and invasion of HT1080 fibrosarcoma cells through inhibiting phosphoinositide 3-kinases independently of autophagy inhibition

SHINGO ITO¹, NOBUKO KOSHIKAWA¹, SHIGENOBU MOCHIZUKI² and KEIZO TAKENAGA¹

Divisions of ¹Chemotherapy and ²Biochemistry, Chiba Cancer Center Research Institute, 666-2 Nitona, Chuoh-ku, Chiba 260-8717, Japan

Received March 12, 2007; Accepted April 26, 2007

Abstract. 3-Methyladenine (3-MA) inhibits class III phosphoinositide 3-kinase (PI3K) and is widely used as an inhibitor of autophagy. 3-MA has also been shown to stimulate cell death of tumor cells under nutrient-starved conditions by inhibiting autophagy. To explore the possibility of this type of autophagy inhibitors as anticancer drugs, we examined the effects of 3-MA on the phenotypes of highly metastatic human fibrosarcoma HT1080 cells. We report here that although 3-MA did not markedly affect cell survival of the cells under either normal or amino acid-starved conditions, it strongly inhibited the invasiveness of the cells. 3-MA rapidly suppressed actin rich membrane ruffle and/or lamellipodia formation under normal conditions, leading to inhibition of cell migration and invasion of the cells without substantial inhibitions of small GTPase Rac activity and the production of matrix metalloproteinases MMP-2 and MMP-9. 3-MA abolished class I and class II PI3Ks in *in vitro* lipid kinase assays, and suppressed cell motility of the cells more strongly than the other PI3K inhibitors wortmannin and LY294002. Downregulation of Beclin 1, a protein required for autophagic body formation, by transfection of Beclin 1 siRNA did not inhibit membrane ruffle formation and cell migration. These results suggest that 3-MA suppresses the invasion of HT1080 cells, independently of autophagy inhibition, through inhibition of type I and II PI3Ks and possibly other molecules.

Introduction

Autophagy is a degradative mechanism mainly involved in the recycling and turnover of cytoplasmic constituents in

eukaryotes, thus is essential for growth regulation and maintenance of homeostasis (1). Defective autophagy causes a number of pathological conditions including vacuolar myopathies, neurodegenerative diseases, liver disease, and some forms of cancer (2). The process is particularly induced when nutrients and/or growth factors are starved. During autophagy, damaged/obsolete cytoplasmic macromolecules and organelles are encapsulated by intracellular vesicles (autophagosomes), which subsequently fused with lysosomes, and are subjected to proteolysis (3). Many important molecules that regulate autophagy have been extensively studied in *Saccharomyces cerevisiae*, especially at genetic level (3), and related homologous proteins have been discovered in mammals including Beclin 1 (4). Beclin 1 forms a complex with class III phosphoinositide 3-kinase (PI3K) and functions at the *trans*-Golgi network (5). It is monoallelically deleted in human sporadic breast cancer, ovarian cancer, and prostate cancer (4). Moreover, Beclin 1^{+/−} mutant mice show a high incidence of spontaneous tumors and decreased autophagy (6).

There are several pharmacological inhibitors of autophagy. One of the most widely used inhibitor is 3-methyladenine (3-MA). It stops autophagy at the sequestration step in mammalian cells through inhibiting class III PI3K without markedly affecting protein synthesis or ATP levels (7-10). Recent studies have shown that 3-MA induces mucopolipidoses type IV (11), inhibits formation of Francisella-containing vacuoles (12), blocks growth factor-withdrawal- and HIV-envelope glycoproteins-induced apoptotic process in CD4⁺ T cells (13,14), and suppresses amyloid β -protein in neuroblastoma cells exposed to hyperoxia (15). PI3K inhibitors such as wortmannin (WMN) and LY294002 have also been shown to inhibit autophagy (16).

Recent studies have shown the importance of autophagy in cancer (17,18). When autophagy is inhibited using either chemical inhibitors including 3-MA or by RNA interference knockdown of autophagy molecules including Beclin 1 in tumor cells under nutrient-deprived conditions, the tumor cells undergo apoptosis (9), suggesting that autophagy may prevent the cells from cell death. In contrast, accumulation of autophagic vacuoles has been considered to be a marker of type II (autophagic) cell death as opposed to type I (apoptotic) cell death (18). Many anticancer agents such as etoposide, tamoxifen, rapamycin and ionizing radiation have

Correspondence to: Dr Keizo Takenaga, Division of Chemotherapy, Chiba Cancer Center Research Institute, 666-2 Nitona, Chuoh-ku, Chiba 260-8717, Japan
E-mail: keizo@chiba-cc.jp

Key words: 3-methyladenine, autophagy, PI3K, lamellipodia, migration, invasion

been reported to induce autophagy, implying that autophagy may be a cause of cell death (19). Thus, the role of autophagy in cancer is complicated and is still a subject of debate.

In the present study, to explore the possibility of autophagy inhibitors as anticancer drugs, we treated highly metastatic human fibrosarcoma HT1080 cells under normal and nutrient-starved conditions with 3-MA. We found that although 3-MA only slightly enhances cell death of the cells under amino acid-starved conditions, it strongly suppresses their motility and invasion under normal culture conditions, thus implicating the application of this type of drugs to prevent invasion and metastasis.

Materials and methods

Cells and culture conditions. Human fibrosarcoma HT1080 cells were obtained from Health Science Research Resources Bank, Osaka. They were cultured in Dulbecco's modified Eagle's medium (DMEM) supplemented with 10% fetal bovine serum (FBS) or Hank's balanced salt solution (HBSS) supplemented with 10% dialyzed FBS (amino acid-starved medium).

Assay for apoptosis. Apoptosis was detected by Annexin V staining using Annexin V-EGFP Apoptosis Detection Kit (MBL, Nagoya) according to the manufacturer's instructions.

Visualization of autophagic vacuoles. Cells cultured in glass-bottom culture dishes (MatTeck, Ashland, MA) were incubated with 50 μ M monodansylcadaverine (MDC) (Sigma-Aldrich, St. Louis, MO) in Dulbecco's PBS (DPBS) at 37°C for 10 min (20). After incubation, cells were washed three times with DPBS and immediately observed under an inverted fluorescence microscope (Olympus, Tokyo). Images were captured with a Cool SNAP charge-coupled device camera and processed using RS Image Express image processing software (Nippon Roper, Tokyo).

Immunofluorescent staining of F-actin. Cells on coverslips were fixed with 4% formaldehyde and 5% sucrose in DPBS for 30 min, permeabilized with 0.5% Triton X-100 in DPBS for 3 min, and then incubated with 3% bovine serum albumin and 0.1% glycine in DPBS for 1 h. For staining F-actin, the cells were incubated with Alexa Fluor[®] 568 phalloidin (Molecular Probe, Eugene, OR) for 30 min at room temperature. For staining Beclin 1, the cells were incubated with polyclonal anti-Beclin 1 antibody (Santa Cruz Biotechnology, Inc., Santa Cruz, CA), washed with DPBS, and then incubated with FITC-labeled goat anti-rabbit IgG. After rinsing, the coverslips were mounted in 50% glycerol in DPBS containing 1 mg/ml *p*-phenylenediamine to inhibit photobleaching.

Migration and invasion assays. Cell motility was measured by using 8- μ m pore size FluoroBlok transwell chambers (BD Sciences Labware, Franklin Lakes, NJ). Cells were collected by a brief treatment with trypsin/EDTA solution, washed once with serum-containing DMEM, centrifuged, resuspended in DMEM containing 0.1% bovine serum albumin, and then placed in the inserts at a concentration of 5×10^4 cells/200 μ l. In the lower compartment of the chamber, 750 μ l of DMEM

containing 10% FBS was added as a chemoattractant. Invasion assay was carried out by the same procedure except that the filters of the transwell chambers were coated with 30 μ g Matrigel (Invitrogen Corp., Carlsbad, CA). After incubation at 37°C for 10 h (migration assay) or 24 h (invasion assay), HT1080 cells that migrated through the pores to the lower chamber were stained with 1 μ M Calcein AM (Molecular Probe) for 10 min and observed under a confocal laser microscope. In migration assays, the number of cells, which had migrated through the membranes, was counted on the pictures of at least three randomly selected fields. In invasion assays, all cells that had invaded through the Matrigel-coated membranes were counted.

Preparation of conditioned media and gelatin zymography. Cells (3×10^5 cells/ml serum-free DMEM) were seeded onto 24-well tissue culture wells in the presence or absence of 10 mM 3-MA. The conditioned medium was collected 24 h after seeding and analyzed for gelatin degrading activity by electrophoresis under non-reducing conditions on 9% SDS-polyacrylamide gels containing 1 mg/ml gelatin. The volume of conditioned medium loaded per lane was standardized on the basis of cell number. After electrophoresis, the gels were washed twice with 200 ml of 2.5% (v/v) Triton X-100 for 1 h at room temperature to remove SDS and then incubated at 37°C overnight in 50 mM Tris-HCl, pH 7.5, 200 mM NaCl, 5 mM CaCl₂ and 0.02% (w/v) Brij-35. The gels were stained with 0.5% (w/v) Coomassie Brilliant Blue R-250 in 30% (v/v) methanol, 10% (v/v) acetic acid, and destained in the same solution without dye.

Transfection of Beclin 1 siRNA. siRNA mediated silencing of endogenous expression of Beclin 1 was performed using Beclin 1 siRNA (Santa Cruz Biotechnology). Beclin 1 siRNA was transfected with Lipofectamine 2000 according to the manufacturer's instructions (Invitrogen). Briefly, one day before transfection, cells were resuspended in 12-well plates in growth medium and then grown overnight. On the day of the experiment, siRNA-Lipofectamine 2000 complexes were prepared and transfection was performed according to the manufacturer's instructions. The cells were transfected with Beclin 1 siRNA for at least 5 h at 37°C before switching to fresh Opti-MEM containing 10% FBS and incubated overnight. The medium was then changed to DMEM supplemented with 10% FBS. As a control for Beclin 1 siRNA, Silencer Negative Control #1 siRNA (Ambion Inc., Austin, TX) was transfected.

Immunoblot analyses. Cells were lysed in 1% Triton X-100, 1% sodium dodecylsulfate, 0.1% SDS, 10 mM Tris-HCl, pH 7.4, 300 mM NaCl, 1 mM EDTA and 1 mM PMSF. After centrifugation at 10,000 g for 10 min at 4°C, the supernatant was used for immunoblot analysis. Proteins were separated by SDS-PAGE under reducing conditions and transferred to a nitrocellulose membrane. After blocking with 5% dry milk in TBS-T (150 mM NaCl, 50 mM Tris-HCl, pH 7.4, and 0.05% Tween-20), the membrane was incubated with polyclonal anti-Beclin 1 antibody (Santa Cruz Biotechnology) or monoclonal anti-phospho-Akt (Ser473) antibody or anti-Akt antibody (Cell Signaling, Danvers, MA), washed extensively

with TBS-T, and then incubated with horseradish peroxidase conjugated secondary antibodies. Immunodetection was carried out using the enhanced chemiluminescence system (ECL, Amersham Biosciences Corp., Buckinghamshire, UK). For a loading control, the membrane was stripped and reprobed with monoclonal anti- β -actin antibody (Sigma-Aldrich).

Rac activation assay. After 3-MA treatment, the cells were washed twice with DPBS and lysed in lysis buffer (50 mM Tris-HCl, pH 7.5, 10 mM $MgCl_2$, 0.5 M NaCl, 1% Triton X-100). The cell lysates were centrifuged at 10,000 g for 10 min at 4°C, and the resultant supernatants (500 μ g proteins) were incubated with PAK-PBD-GST fusion protein beads (Cytoskeleton, Inc., Denver, CO) at 4°C overnight. The beads were washed twice with the lysis buffer followed by two washings with wash buffer (25 mM Tris-HCl, pH 7.5, 30 mM $MgCl_2$, 0.5 M NaCl). The activated GTP-bound forms of Rac bound to beads and total Rac in cell lysates were detected by immunoblot using monoclonal anti-Rac1 antibody (BD Biosciences, San Jose, CA), as described above.

Analysis of PI3K activity. Class I, class II and class III PI3K activities were analyzed as described previously (21). Briefly, for analysis of class I PI3K activity, cells were washed with ice-cold buffer A (50 mM HEPES, pH 7.4, 150 mM NaCl, 10 mM EDTA, 10 mM $Na_4P_2O_7$, 100 mM NaF and 2 mM Na_3VO_4), and extracted for 15 min at 4°C with buffer A supplemented with 0.5 mM PMSF, 1% Nonidet P-40 (NP-40) and protease inhibitor cocktail (Roche Diagnostics, Mannheim). After centrifugation at 10,000 g for 10 min at 4°C, the supernatants were immunoprecipitated with polyclonal anti-p85 class I PI3K (Santa Cruz Biotechnology) and Protein A-Sepharose beads for 2 h at 4°C. The beads were washed twice with 1% NP-40 in DPBS, twice with 0.5 M LiCl in 100 mM Tris-HCl (pH 7.4), and twice with 100 mM NaCl and 1 mM EDTA in 10 mM Tris-HCl (pH 7.4). The beads were resuspended in 30 μ l buffer 1 (20 mM HEPES, pH 7.5, 0.4 mM EGTA and 0.4 mM Na_2HPO_4), and supplemented with 10 μ l pre-sonicated phosphatidylinositol (PtdIns) (1 μ g/ μ l) (Biomol, Plymouth Meeting, PA) in 5 mM HEPES (pH 7.5). The lipid kinase assay was started by adding 10 μ l of buffer 1 supplemented with 1 μ Ci/ μ l [γ - ^{32}P]ATP (GE Healthcare Bio-Sciences Corp., Piscataway, NJ), 250 μ M ATP- Na_2 and 50 mM $MgCl_2$. After 15-min incubation at 37°C, the reactions were stopped by adding 15 μ l of 4 M HCl. Phospholipids were extracted with 130 μ l of chloroform/methanol (1:1, v/v) and separated on Silica Gel 60A (Merck KGaA, Darmstadt) with chloroform/methanol/4.3 M ammonia (9:7:2, v/v/v). Phospholipids were identified by comparison with unlabeled phosphoinositide after exposure to iodine vapour. Radiolabeled PtdIns3P was detected by autoradiography. For analysis of class II PI3K, cells were disrupted by successive pumpings through a 26-gauge needle in 20 mM Tris-HCl (pH 7.4), 125 mM NaCl, 0.2 mM EGTA, 0.2 mM EDTA, 1 mM Na_3VO_4 and protease inhibitor cocktail. After centrifugation of the cell lysates at 2,500 g for 10 min at 4°C, the supernatant was further centrifuged at 100,000 g for 2 h at 4°C. The resultant pellet was resuspended in buffer 2 (20 mM Tris-HCl, pH 7.4, 125 mM NaCl, 0.2 mM EGTA and 0.2 mM EDTA),

and 30 μ l aliquots were supplemented with 10 μ l of sonicated PtdIns (1 μ g/ μ l) and pre-incubated for 10 min. The reaction was started by adding 10 μ l of 20 mM Tris-HCl, pH 7.4, 125 mM NaCl, 1 μ Ci/ μ l [γ - ^{32}P]ATP, 250 μ M ATP- Na_2 and 25 mM $CaCl_2$. After a 15-min incubation at 37°C, phospholipids were analysed as described above. For analysis of class III PI3K, cells were lysed in 20 mM Tris-HCl, pH 7.4, 130 mM NaCl, 1 mM EDTA, 1 mM Na_3VO_4 , 1 mM PMSF, 1% Triton X-100 and protease inhibitor cocktail for 15 min at 4°C. After centrifugation at 10,000 g for 10 min at 4°C, the supernatants were immunoprecipitated with polyclonal anti-class III PI3K (Abcam, Cambridge) and protein A-Sepharose for 2 h at 4°C. The beads were washed twice with the lysis buffer, and once with buffer 3 (20 mM Tris-HCl, pH 7.4, 130 mM NaCl and 0.2 mM EDTA). The beads were re-suspended in 30 μ l of buffer 3 supplemented with 10 μ l of sonicated PtdIns (1 μ g/ μ l) and pre-incubated for 10 min. The reactions were started by adding 10 μ l of buffer 3 supplemented with 1 μ Ci/ μ l [γ - ^{32}P]ATP, 250 μ M ATP- Na_2 and 25 mM $MnCl_2$. After a 15-min incubation at 37°C, phospholipids were analysed as described above.

Results

Effect of 3-MA on cell survival of HT1080 cells under normal and amino acid-starved conditions. First, we examined the status of autophagy in HT1080 cells under normal culture conditions. For this, the cells were incubated with the auto-fluorescent drug MDC, a specific autophagosome marker (20). We used HeLa cells as a reference because they are reported to be sensitive to and induced to die by 3-MA (10). The staining revealed that both cell types contained many MDC-labeled vacuoles in the cytoplasm (Fig. 1A). This result prompted us to test whether inhibition of autophagy affects cell survival of HT1080 cells under normal and amino acid-starved conditions. HT1080 cells were cultured in DMEM or HBSS (amino acid-starved) for 48 h in the presence or absence of 10 mM 3-MA, at which concentration autophagy has been shown to be blocked (7-15). As shown in Fig. 1B, 3-MA only slightly enhanced cell death of HT1080 cells under normal conditions while it markedly stimulated that of HeLa cells (Fig. 1B). Supporting these results, apoptosis was not induced by 3-MA in HT1080 cells by 24 h after the treatment while it was markedly induced in HeLa cells (Fig. 1C). Under amino acid-starved conditions, both HT1080 and HeLa cells died to some extent within 48 h. Again, 3-MA only slightly enhanced cell death of HT1080 cells (Fig. 1B). Thus, HT1080 cells were refractory to 3-MA compared to HeLa cells. We also examined the sensitivity of mammary carcinoma MDA-MB-231 and pancreatic carcinoma AsPC-1 cells to 3-MA and found that they were quite insensitive to 3-MA even under starved conditions (data not shown).

3-MA inhibits membrane ruffle formation in HT1080 cells under normal culture conditions. Although 3-MA did not significantly affect cell survival of HT1080 cells for at least 24 h under normal culture conditions, we noticed that it induced morphological changes accompanied by a significant reduction of membrane ruffle and/or lamellipodia formation

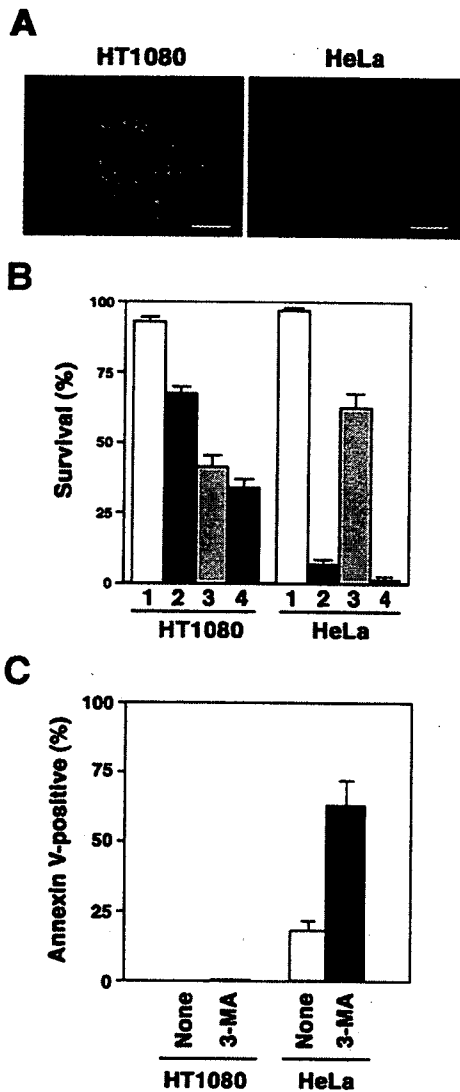


Figure 1. Effect of 3-MA on cell survival. (A) MDC-labeled autophagic vacuoles in HT1080 and HeLa cells under normal growth conditions. Pseudocolored. Scale bar, 20 μ m. (B) Cell survival. HT1080 and HeLa cells were cultured in DMEM/10% FBS (normal medium) (columns 1 and 2) or HBSS/10% dialyzed FBS (amino acid-starved medium) (columns 3 and 4) in the absence (columns 1 and 3) or presence of 10 mM 3-MA (columns 2 and 4) for 48 h. Cell viability was determined by trypan-blue staining. Bars, SD. (C) Apoptosis. HT1080 and HeLa cells were cultured in normal medium with or without 10 mM 3-MA for 24 h. The number of annexin V-positive cells was counted. Bars, SD.

(Fig. 2A and B). This was more clearly observed after staining F-actin with Alexa Fluor 568 phalloidine. The reduction in actin rich membrane ruffle formation was detected as early as 30 min after 3-MA treatment and further pronounced as the treatment time prolonged (Fig. 2C-F). HT1080 cells inherently have poorly organized actin stress fibers, and the actin stress fibers were further disorganized by 3-MA.

3-MA inhibits cell motility of HT1080 cells under normal culture conditions. Since membrane ruffle and/or lamellipodia formation is generally an indicator of cell migration, we examined the migratory ability of 3-MA-treated HT1080 cells. To this end, we employed Transwell migration assay in which FBS was used as a chemoattractant. Counting of the

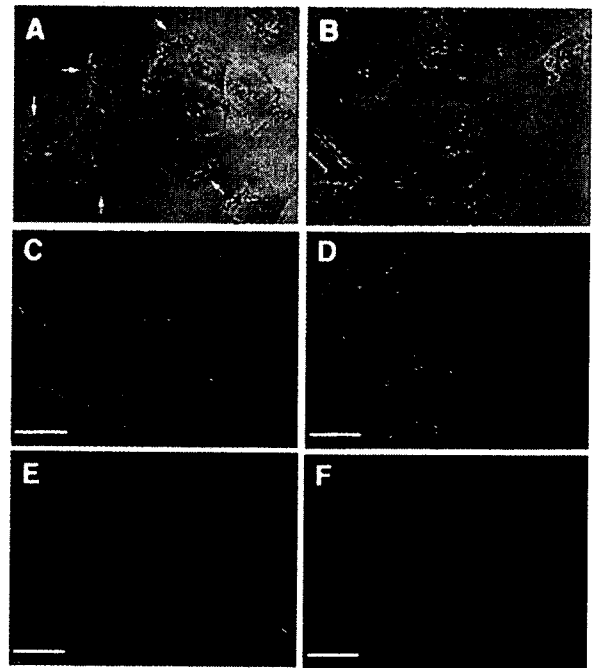


Figure 2. Effect of 3-MA on membrane ruffle formation. (A and B) Phase contrast images of HT1080 cells. The cells were cultured in the absence (A) or presence (B) of 10 mM 3-MA for 8 h. Arrows indicate membrane ruffles and/or lamellipodia. (C-F) HT1080 cells were cultured in the absence (C) or presence of 10 mM 3-MA for 0.5 h (D), 1 h (E) or 2 h (F). The cells were stained with Alexa Fluor 568 phalloidine, and then observed under a confocal laser microscope. Scale bar, 50 μ m.

cells that migrated through the pores to the lower surface of the filters during a 10-h incubation period revealed that 3-MA (5-10 mM) strongly inhibited cell migration (Fig. 3A). 3-MA also inhibited cell migration of human lung adenocarcinoma A549 and MDA-MB-231 cells (data not shown), suggesting that 3-MA inhibits the migration of a variety of cell lines.

Small GTPase Rac is an important effector of PI3K and has been found to regulate membrane ruffle and/or lamellipodia formation and cell motility (22). To examine whether 3-MA treatment could reduce Rac activity, we treated HT1080 cells with 10 mM 3-MA for up to 2 h, and the intracellular concentration of the active GTP-bound form of Rac was measured. The data showed that 3-MA did not change the amount of GTP-Rac (Fig. 3B).

We next compared the effect of 3-MA on cell migration with those of WMN and LY294002. As show in Fig. 3C, both 100 nM WMN and 25 μ M LY294002 suppressed cell migration of HT1080 cells, in agreement with the previous report (23). However, their effect was weaker than that of 10 mM 3-MA.

3-MA inhibits the invasion of HT1080 cells. The above results suggested that 3-MA could inhibit the invasion of HT1080 cells. Then we performed Matrigel invasion assays, and found that it significantly inhibited the invasive ability of the cells (Fig. 4A).

To test whether 3-MA affects the secretion of MMPs, which are essential for tumor cells to invade, we carried out gelatin zymography. Results showed that HT1080 cells secreted three major MMP activities (assigned as proMMP-9,

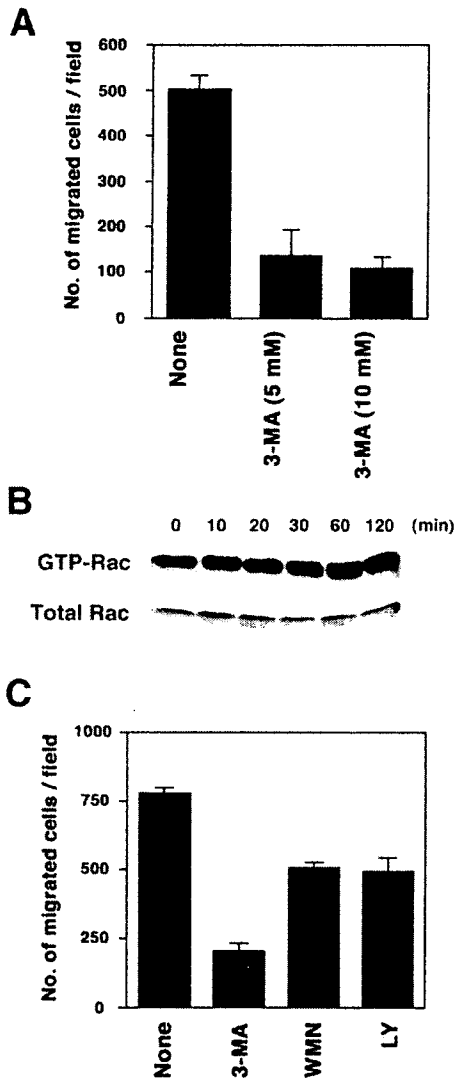


Figure 3. Effects of 3-MA on cell migration. (A) Migration assay. HT1080 cells were subjected to transwell migration assays in the absence or presence of 5 mM or 10 mM 3-MA for 10 h. The number of migrated cells was counted on the pictures of at least three randomly selected fields. Bars, SD. (B) Pull-down assay of activated Rac. The GTP-bound form of Rac was pulled down with GST fusion proteins, corresponding to the p21-binding domain (PBD) of human PAK-1, conjugated to agarose beads. The GTP-Rac proteins bound to the beads were identified using anti-Rac antibody by Western blotting. Cell lysates were also subjected to immunoblot analysis to detect Rac. (C) Comparison of the inhibitory effect of 3-MA, WMN and LY294002 on cell migration. HT1080 cells were subjected to transwell migration assays in the absence or presence of 10 mM 3-MA, 100 nM WMN or 25 μ M LY294002 (LY). Bars, SD.

proMMP-2 and activated MMP-2, based on size) into the culture medium, which are completely abolished in the presence of the MMP inhibitor 1, 10-phenanthroline (Fig. 4B). 3-MA slightly suppressed the secretion of proMMP-9, but showed virtually no effect on the secretion of proMMP-2 and activated MMP-2. Thus, the inhibition of invasion by 3-MA is likely to be due to the suppression of cell motility.

Downregulation of Beclin 1 does not suppress cell migration of HT1080 cells. To examine whether autophagy inhibition itself is associated with the suppression of membrane ruffling and cell motility, we transfected Beclin 1 siRNA into HT1080

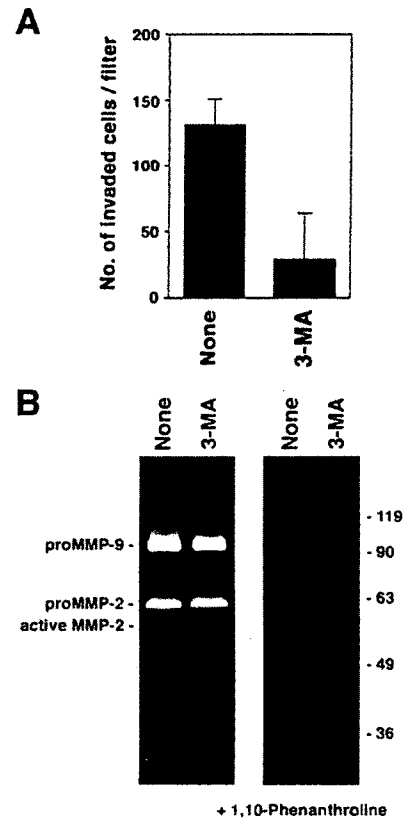


Figure 4. Effects of 3-MA on invasion and MMP secretion. (A) Invasive ability. HT1080 cells were subjected to Matrigel invasion assays in the absence or presence of 10 mM 3-MA for 24 h. All the cells that had invaded through the Matrigel-coated membranes were counted. Bars, SD. (B) MMP secretion. HT1080 cells were cultured for 24 h in the absence or presence of 10 mM 3-MA. MMPs secreted into the conditioned medium were analyzed by gelatin zymography. 1, 10-Phenanthroline was used as an MMP inhibitor.

cells. Immunoblot analysis demonstrated that the expression of Beclin 1 was suppressed by the siRNA (Fig. 5A). As expected, the number of cells with MDC-labeled vacuoles was decreased in the siRNA-transfected cells (Fig. 5B). Immunofluorescent staining showed that Beclin 1 was concentrated at the perinuclear region (Fig. 6), consistent with the previous report (5). Transfection of Beclin 1 siRNA resulted in the disappearance of perinuclear staining. However, membrane ruffle formation was still observed in the Beclin 1 knockdown cells (Fig. 6). Furthermore, the migratory ability of the cells was completely refractory to the siRNA treatment (Fig. 5C).

3-MA inhibits class II PI3K as well as class I and III PI3Ks. 3-MA is known to directly inhibit class III PI3K (8,16). It was also demonstrated to inhibit phosphorylation of ribosomal S6 protein, suggesting the inhibition of class I PI3K (16). To obtain information about the mechanism underlying the inhibition of cell motility by 3-MA, we carried out *in vitro* PI3K activity assays, according to the previous protocol (21), especially focusing on the effect on class II PI3K activity. Results showed that 10 mM 3-MA inhibited class III PI3K as potent as 100 nM WMN (Fig. 7A). 3-MA also inhibited class I PI3K as effective as 100 nM WMN. This was further corroborated by the inhibition of phosphorylation of Akt, a downstream target of class I PI3K. 3-MA inhibited Akt